

New bedrock geology of Mount Mervyn map sheet (106C/04) and mineral potential for the South Wernecke mapping project

Joyia Chakungal¹ and Venessa Bennett
Yukon Geological Survey

Chakungal, J. and Bennett, V., 2011. New bedrock geology of Mount Mervyn map sheet (106C/04) and mineral potential for the South Wernecke mapping project. *In: Yukon Exploration and Geology 2010*, K.E. MacFarlane, L.H. Weston and C. Relf (eds.), Yukon Geological Survey, p. 55-87.

ABSTRACT

An integrated bedrock mapping and regional soil sampling program in the Mount Mervyn map area (106C/04) was undertaken in 2010. It is the first year of a multi-year initiative called the South Wernecke mapping project (SWP), which will cover ten 1:50K map sheets in the southern Wernecke Mountains area in central Yukon. Field work in the first year served to highlight the complexities of the bedrock geology in the region, and identify areas of mineral potential.

The Mount Mervyn map sheet is underlain by Proterozoic and Paleozoic siliciclastic and carbonate rocks that have been deformed into an east-trending fold-and-thrust belt. Regional soil geochemical data coupled with bedrock observations highlight new areas of mineral potential (*i.e.*, Ni and Au) that have not been previously identified.

¹joyia.chakungal@gov.yk.ca

INTRODUCTION

In 2010, the Yukon Geological Survey initiated a multi-year mapping program entitled the South Wernecke mapping project (SWP). A core objective of the project is aimed at updating geoscience information available for an area spanning ten 1:50K map sheets in the southern Wernecke Mountains of central Yukon (Figs. 1a,b). The area of interest is situated northeast of the Tintina Fault and includes rocks of the Proterozoic western margin of ancestral North America on which the Paleozoic Selwyn basin subsequently formed. More specifically, the study area is inferred to straddle the boundary between siliciclastic rocks of the Selwyn basin and correlative platform carbonates that unconformably overlie Paleo - Neoproterozoic basement (Fig. 1c). The map area also includes the recently discovered Rackla Gold Belt, a phrase coined by ATAC Resources (property holders), that lies within a structural corridor bounded by the Kathleen Lakes Fault on the north and the Dawson thrust on the south.

Over the next several years the SWP will upgrade the stratigraphy of the area to a standard comparable to that of western Yukon (Fig. 2) and eastern Northwest Territories (NWT), and document the structural elements in order to better understand the area's tectonic evolution. In particular, structures that may have facilitated or controlled development of precious and polymetallic mineral deposits in the area will be examined. A longer-term goal of the SWP is to support regional correlations across Alaska, Yukon, and NWT by integrating the results of this study with work being undertaken across the region by university-based colleagues (Fig. 1; Macdonald *et al.*, this volume; Medig *et al.*, 2010; Nielsen and Thorkelson, this volume; Peters and Thorkelson, this volume; Thiessen and Gleeson, in progress; Turner, this volume). With these goals in mind, field investigations during the summer of 2010 were carried out over six weeks with limited helicopter support. Work was conducted out of eight fly camps positioned throughout the 1:50K Mount Mervyn map sheet (106C/04).

In the following contribution we briefly outline the regional geological context and mineral potential before presenting results of the 2010 bedrock mapping program that was aimed at updating the existing 1:250K map (Blusson, 1974) to 1:50K. Additionally, we report results of a YGS pilot study designed to assess the practical and

scientific feasibility of completing regional soil sampling concurrently with regional bedrock mapping.

GEOLOGICAL SETTING

In north and central Yukon, Paleo and Neoproterozoic sedimentary and volcanic rocks of Laurentian affinity are exposed in a series of inliers in the Wernecke and Ogilvie mountains (Fig. 1a). The Selwyn basin, which overlaps the western margin of Laurentia, comprises a sequence of deep-water sediments that range from latest Neoproterozoic to middle Devonian age. Correlative platform rocks associated with the basin unconformably overlie Laurentian basement in the Wernecke and Ogilvie mountains, and give way southward to the deep-water clastic rocks south of the Dawson thrust. Basement rocks on which the deep water sediments of the Selwyn basin have been deposited are unknown. Recent and ongoing research across northern Yukon permit regional stratigraphic correlations between inliers, except in the south Wernecke Mountains where a lack of data preclude such correlations.

While stratigraphic details and associated nomenclature differ from west to east across the Coal Creek, Hart River, and Wernecke inliers, a number of units are common to all three (Fig. 2). From oldest to youngest, Laurentian basement rocks include:

1. Rift-related Paleoproterozoic rocks of the Wernecke Supergroup;
2. Meso - Neoproterozoic rift-related rocks (Pinguicula Group in the Wernecke and Hart River inliers; Fifteenmile Group in the Coal Creek inlier; Mackenzie Mountain supergroup (Wernecke and Northwest Territory);
3. Rift-related (opening of Pacific Ocean at ~ 700 Ma) early Neoproterozoic Windermere Supergroup.

Overlying supracrustal sequences of the Laurentian basement are upper Neoproterozoic - middle Devonian rocks of the Selwyn basin. Lithologies include basinal sediments (Hyland, Gull Lake and Road River groups) and correlative platform carbonate rocks. Stratigraphically overlying sedimentary rocks of the Selwyn basin are late Devonian rift-related clastic rocks of the Earn Group, terrigenous Triassic and younger sedimentary rocks.

Descriptions of the above units and their structural geometry as observed in the Mount Mervyn area are discussed in the bedrock section below.

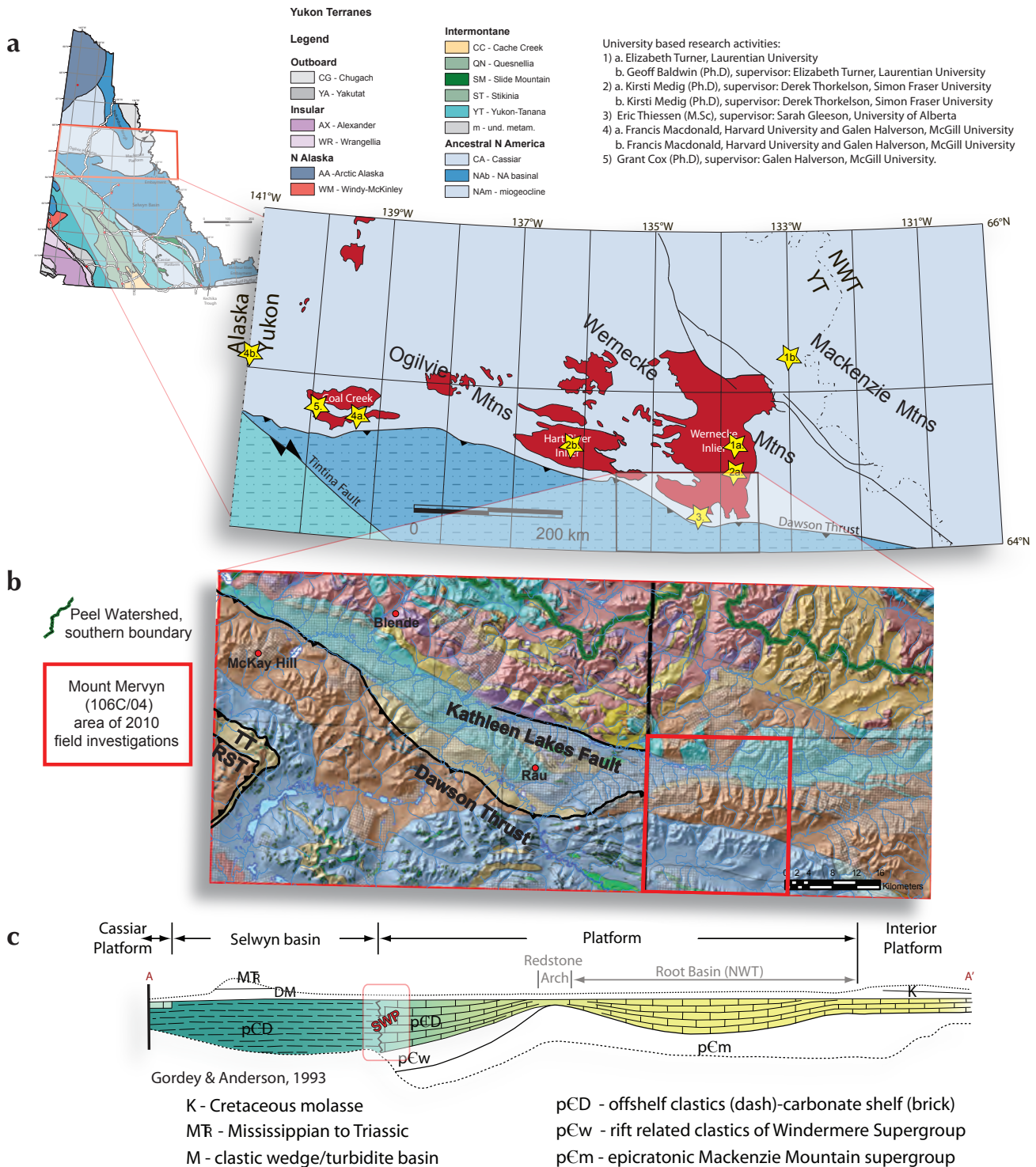


Figure 1. (a) Terrane map for the central Yukon, highlighting in red the distribution of inliers in which Proterozoic 'basement' rocks are exposed. Yellow stars indicate locations for university based research activities. (b) Regional compilation map of Gordey and Makepeace (2001) for the South Wernecke mapping project and surrounding area. Red circles indicate the position of current exploration targets. The focus of 2010 field work is highlighted by the red box (1:50K, 106C/04). Legend: TT, Tombstone Thrust; RST, Robert Service Thrust. (c) A southwest oriented cross-section that extends from the Paleozoic Mackenzie platform in Northwest Territories, westward into Yukon and the Selwyn basin. The South Wernecke Project (SWP) area straddles the northern boundary between siliciclastics of the Selwyn basin and correlative platform carbonates that sit unconformably on Paleo - Neoproterozoic basement.

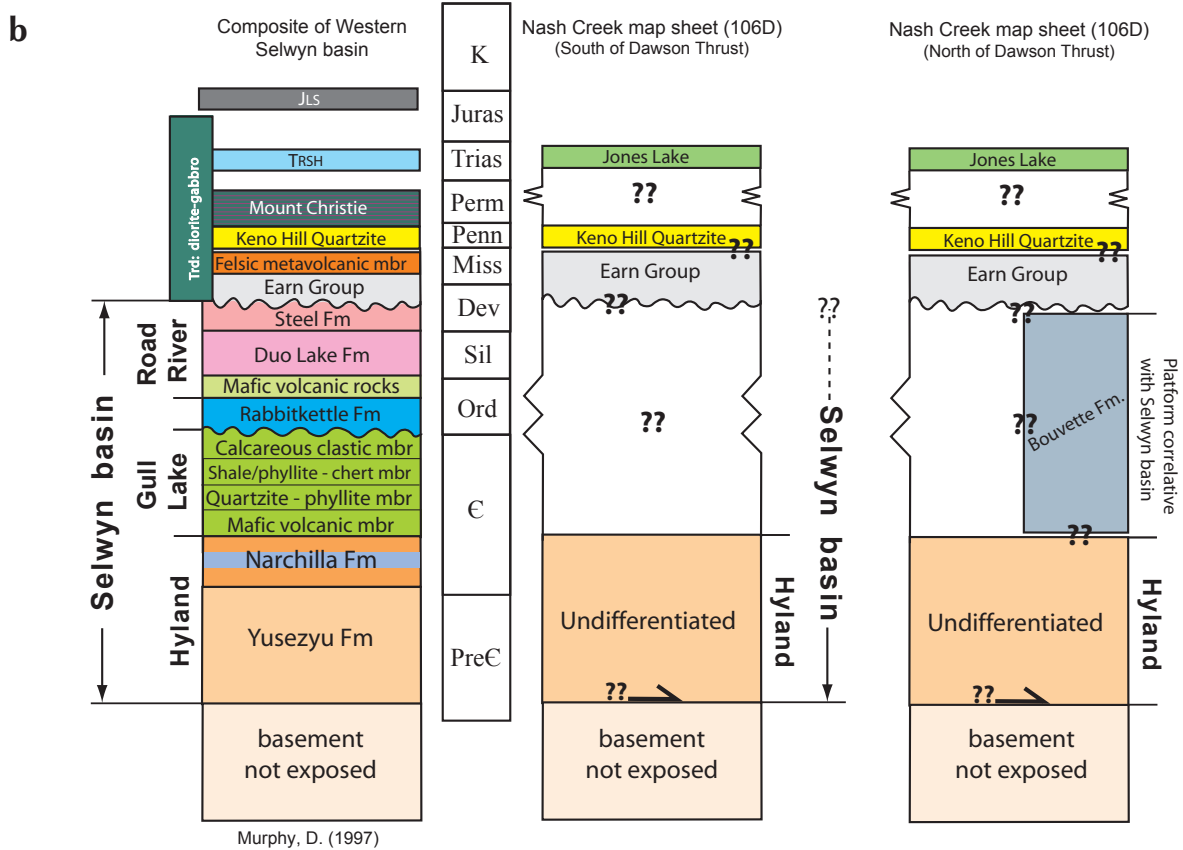
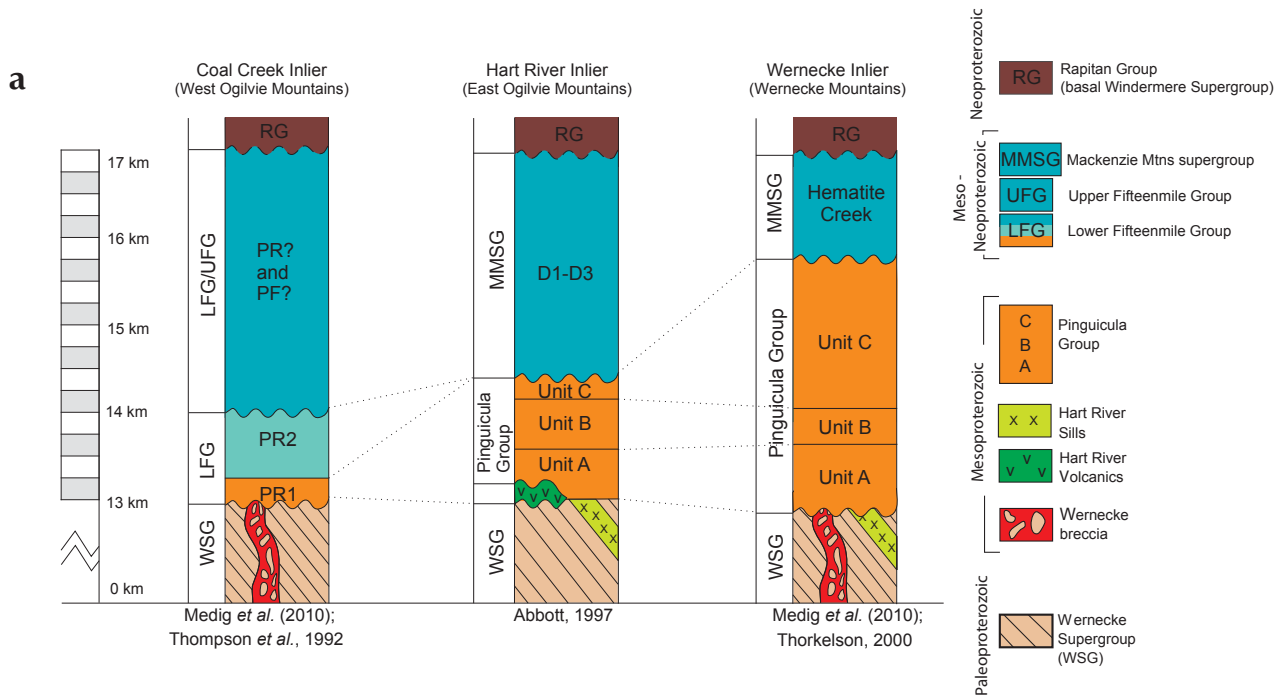


Figure 2. (a) Stratigraphic correlation charts for Paleoproterozoic – Neoproterozoic stratigraphy across the Yukon, and (b) stratigraphic column for Neoproterozoic through to Paleozoic stratigraphy in west Yukon as compared to the current stratigraphic understanding of coeval rocks in the area of interest to the South Wernecke mapping project.

REGIONAL MINERAL POTENTIAL

The SWP is host to a diverse range of mineralization styles. Sixty-five Yukon MINFILE showings, drilled prospects and deposits occur within the footprint of the project area (Yukon MINFILE, 2010). Showings include northeastern extensions of the Ag-Pb-Zn vein faults of the Keno Hill camp (within 106D/03), the Cu-Pb-Ag-Zn Marg deposit (Yukon MINFILE 106D 009), the Pb-Zn-Ag Blende deposit (Yukon MINFILE 106D 064), the past producing polymetallic vein systems of McKay Hill (Yukon MINFILE 106D 038) and the newly discovered and drilled Au prospect of the Rau property (Yukon MINFILE 106D 098; Fig. 3). Importantly, south and west of the project area (1:50K sheets: 106D/04, 105M/13 and 105M/14), the region is host to the high-grade, past and current-producing Ag-Pb-Zn veins of the Keno Hill mining camp, and Au and W deposits at Dublin Gulch, which is at the pre-feasibility stage of project development (Eagle Au deposit, Yukon MINFILE 106D 025, and Mar Tungsten, Yukon MINFILE 106D 027; Fig. 3).

Among the MINFILE occurrences located in the SWP area, three main mineralization styles are recognized

and broadly correlate to host lithology. These styles include: (i) Mississippi Valley-type Ag-Pb-Zn occurrences associated with both Proterozoic and Paleozoic carbonate units; (ii) Syngenetic sedimentary exhalative (SEDEX) and volcanogenic massive sulphide (VMS) occurrences that are host to significant barite, Pb-Zn-Ag and Cu, and interpreted to have formed in Devonian – Mississippian Earn Group and associated volcanic rocks; and (iii) Intrusion-hosted and related $W \pm Cu$ skarn occurrences that relate to surface and near surface occurrences of Cretaceous intrusions belonging to both the Tombstone and McQuesten magmatic suites. A fourth mineralization style is not associated with a specific host lithology but rather with numerous epigenetic polymetallic vein systems that postdate the polydeformed stratigraphy in the area.

Exploration activity in the project area has significantly increased since the discovery of the carbonate-replacement Au prospects of the Tiger and the Osiris zones within the Rau property of ATAC Resources (Yukon MINFILE 106D 098; Figure 3). The discoveries have highlighted the high Au potential of Paleozoic carbonate platform rocks that are both stratigraphically and tectonically intercalated with Selwyn basin stratigraphy.

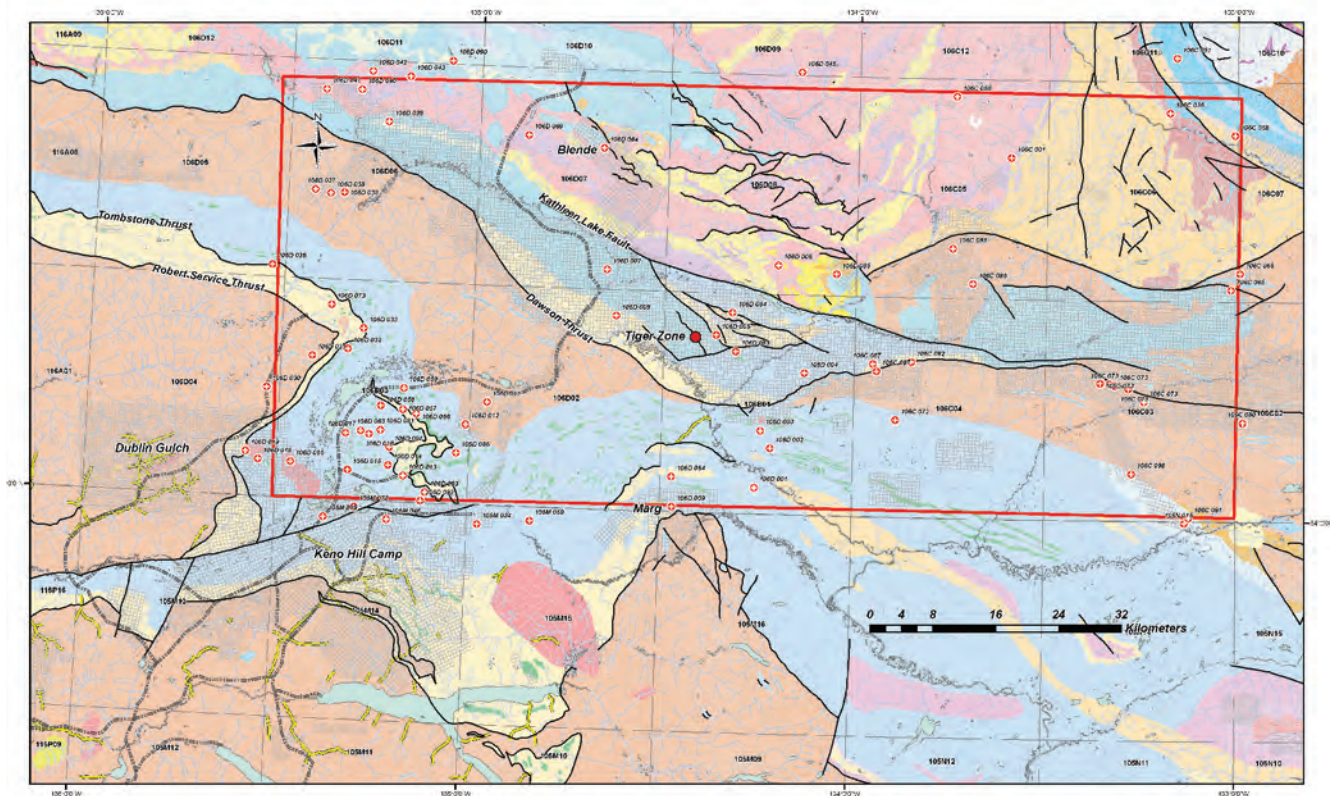


Figure 3. Distribution of Yukon MINFILE showings, drilled prospects and deposits within the South Wernecke bedrock mapping project area. Major regional faults and thrust systems marked. Carbonate hosted gold drilled prospect of the Tiger zone of ATAC resource also marked for reference.

Tiger Zone gold mineralization is associated with thrust imbricated packages of the Silurian – Devonian Bouvette Formation (CD_B) situated in the foot-wall of the Dawson thrust and south of the Kathleen Lakes fault (Fig. 3). In addition to the main sulphide ore body, Au mineralization is also associated with a series of north-striking oxidizing fault zones (ATAC Corporate presentation; December 2010). Continued regional exploration throughout the property has demonstrated a spatial association of Au occurrences to a prominent west-northwest-trending structural corridor located north of the Dawson thrust and south of the Kathleen Lake Fault (Fig. 3). The new Osiris drilled prospect, located ca. 100 km to the east of the Tiger Zone (106C/01), is hosted in a stratigraphically different carbonate package (possibly Cambrian carbonate units associated with the Hyland Group; Fritz *et al.*, 1991) within this regional structural corridor (Fig. 3). Both drilled prospects bear many hallmarks of Carlin-style gold mineralization and consequently the discoveries have resulted in a new staking rush in the region, closely following on the heels of the White Gold staking rush in the Dawson Range.

Analysis of key metals and tracer elements associated with NRCan's Regional Silt Geochemistry (RGS) database (Héon, 2003) within the SWP area has been important for delineating first-order metallogenic domains. The database has also been utilized to identify several areas of significant mineral potential which are currently under explored. Figures 4 –9 represent colour-gradient gridded maps of RGS metal anomalies in the SWP area for Pb, Zn, Cu, Au, W and Mo. Areas in red correspond to 95th percentile (or 2 Standard Deviations) anomalies in the dataset. Integration of RGS data with MINFILE data allow a number of important observations, including:

1. Areas of anomalous Pb (Fig. 4) show a strong spatial correlation with known MVT occurrences. Polymetallic vein systems represent a subordinate contribution to anomalous Pb RGS values.
2. Anomalous Zn domains coincide predominantly with polymetallic vein occurrences (Fig. 5), and to a lesser extent are associated with MVT occurrences and the Marg VMS deposit.
3. Copper anomalies north of the Kathleen Lakes fault coincide spatially with Pb anomalies, in addition to surface occurrences of carbonate hosted MVT mineralization and polymetallic vein prospects (Fig. 6). South of the Kathleen Lakes Fault, domains of anomalous Cu show a stronger spatial correlation with polymetallic vein occurrences. The most anomalous Cu values are associated with drainages proximal to the Marg VMS deposit. Note also that several areas of anomalous Cu are not spatially associated with known mineral occurrences at surface (e.g., within 106D/02 a broad arcuate area of anomalous Cu is defined in the RGS dataset).
4. Elevated Au domains occur within the structural corridor bound by the Dawson Thrust and Kathleen Lakes Fault. Of these, values correlating with the Tiger Zone are most anomalous for gold (Fig. 7). Several Au anomalies are also evident to the north and south of the structural corridor, and are currently not well understood (e.g., two anomalies occur in the Southern and Northern domains of the Mount Mervyn map sheet; Fig. 7).
5. Domains of anomalous W show good correlation with surface occurrences of W ± (Cu) skarn, suggesting W values in the RGS data can be used as a tracer metal for intrusion-hosted and/or related mineralization vectoring (Fig. 8).
6. Five areas of elevated Mo occur in the SWP area, one of which occurs within the Mount Mervyn map sheet and coincides with anomalous Au in the Northern domain (Figs. 7 and 9). The largest anomaly coincides with a strong W anomaly located to the west of the Tiger Zone and immediately south of the Dawson Thrust. Elevated Mo values may correlate with intrusion-related mineralization though a definitive correlation for the remainder of the anomalous regions has yet to be established.

BEDROCK GEOLOGY

STRATIGRAPHY

Field observations permit division of the Mount Mervyn map area into three lithologically and structurally distinct domains herein referred to as the Southern; Central; and Northern domains. Unit descriptions provided below correspond with unit designators as indicated in the legend of Figure 10. Unit names are informal, and are utilized for two reasons: first, not all units are correlated with certainty to stratigraphic units defined by previous workers; and secondly, as noted above, regional stratigraphic correlation studies underway will likely result in revisions to existing nomenclature. As mapping proceeds in the South Wernecke area over the next several years, formal stratigraphic names that are consistent with current nomenclature will be assigned to map units. In the sections below, rocks are tentatively correlated with their named stratigraphic equivalents.

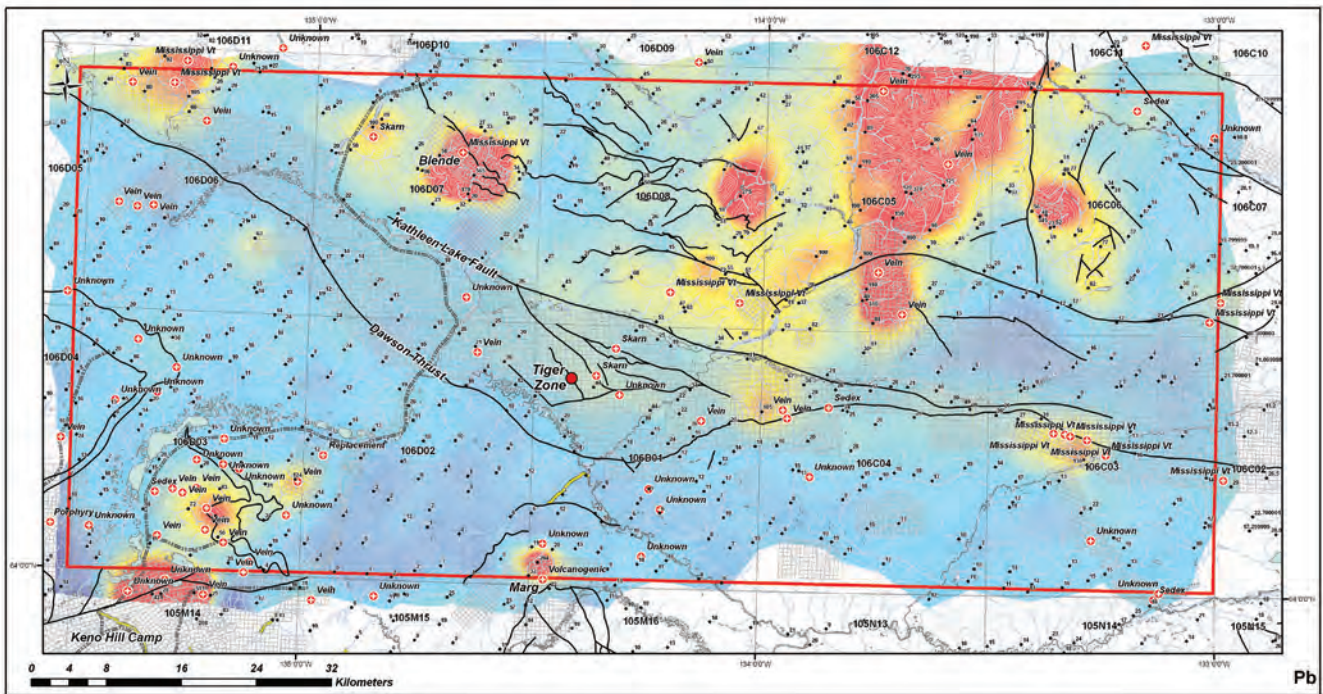


Figure 4. Colour-gradient gridded map of RGS Pb anomalies in the South Wernecke bedrock project area. Areas in red correspond to 95th percentile (or 2 standard deviations) anomalies in the dataset.

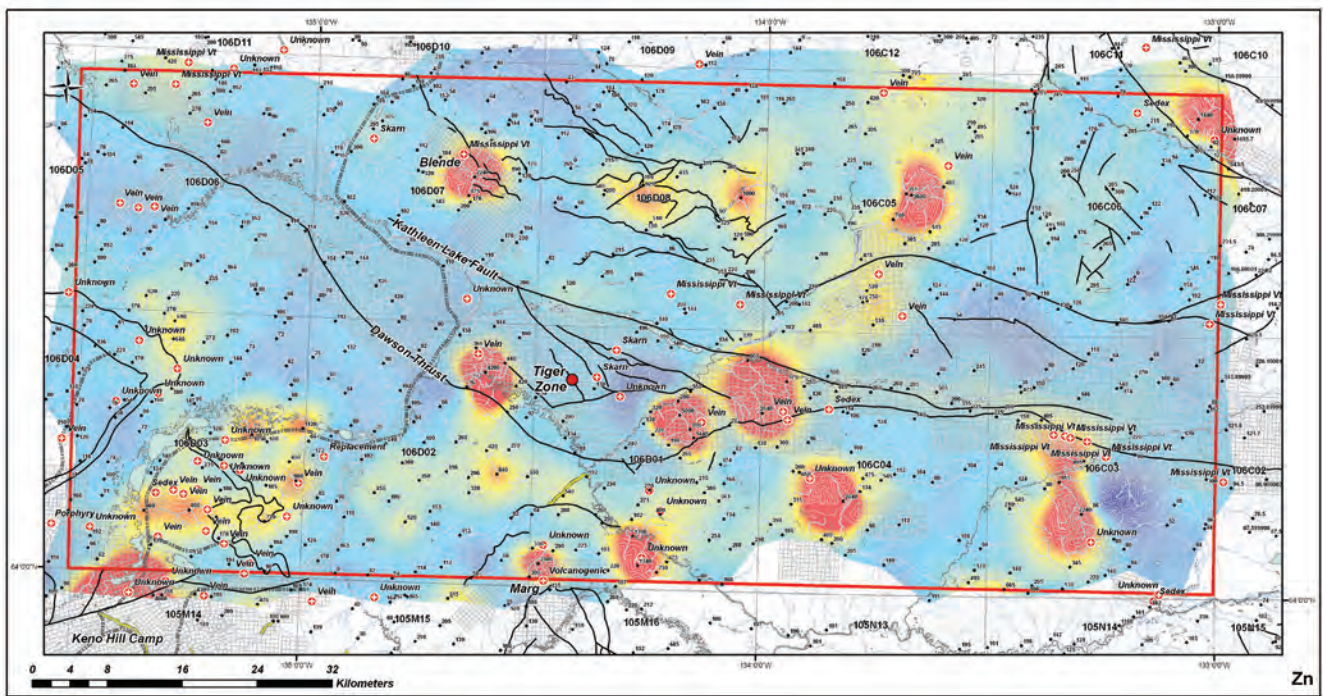


Figure 5. Colour-gradient gridded map of RGS Zn anomalies in the South Wernecke bedrock project area. Areas in red correspond to 95th percentile (or 2 standard deviations) anomalies in the dataset.

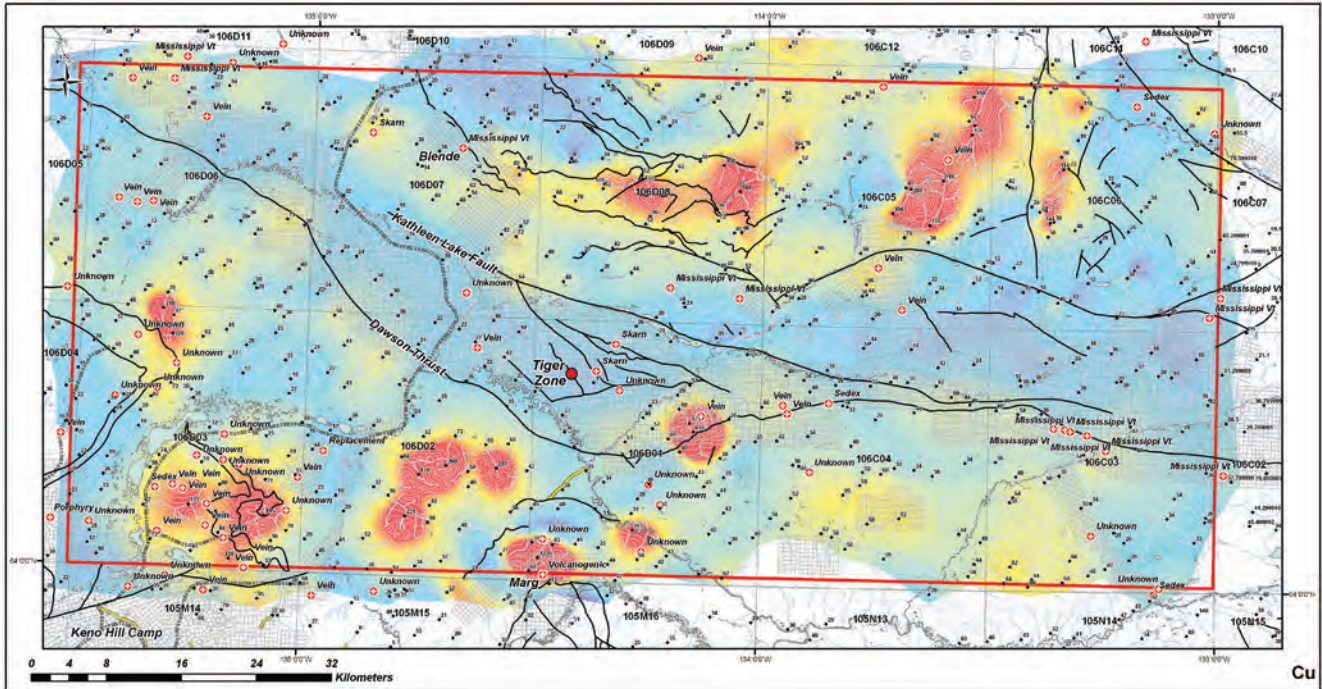


Figure 6. Colour-gradient gridded map of RGS Cu anomalies in the South Wernecke bedrock project area. Areas in red correspond to 95th percentile (or 2 standard deviations) anomalies in the dataset.

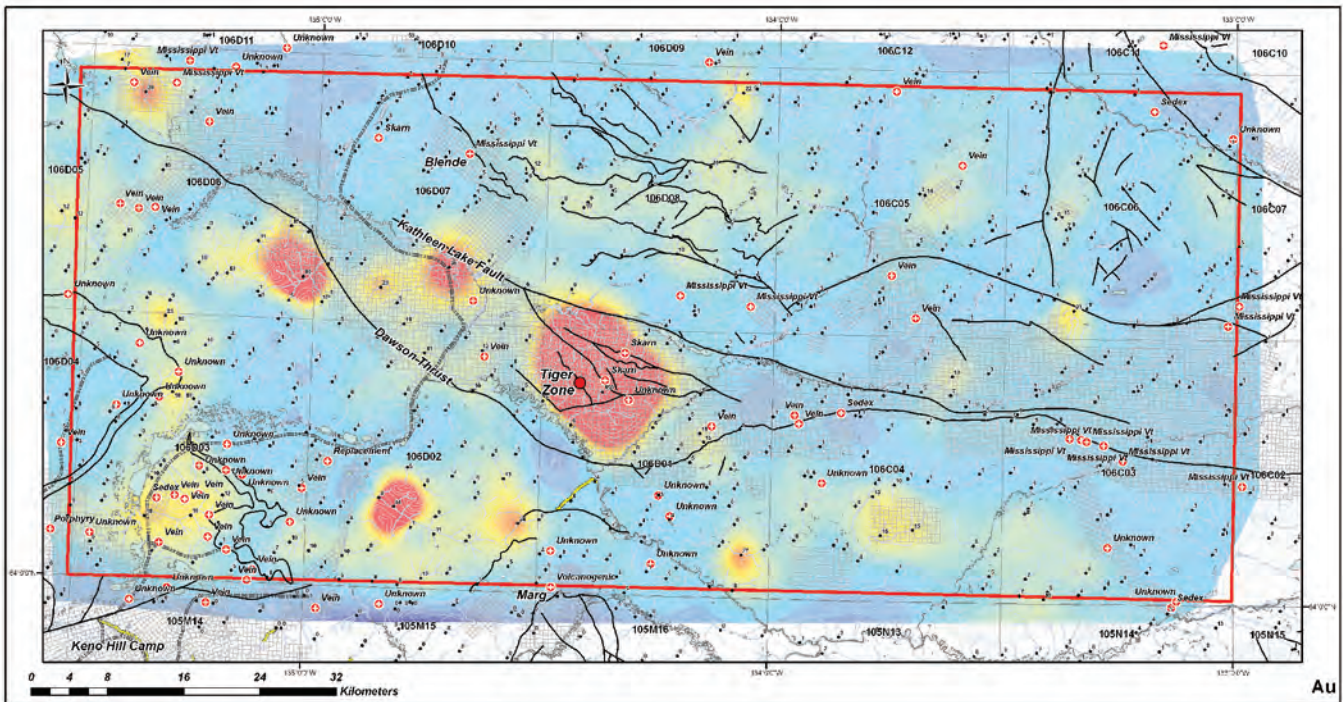


Figure 7. Colour-gradient gridded map of RGS Au anomalies in the South Wernecke bedrock project area. Areas in red correspond to 95th percentile (or 2 standard deviations) anomalies in the dataset.

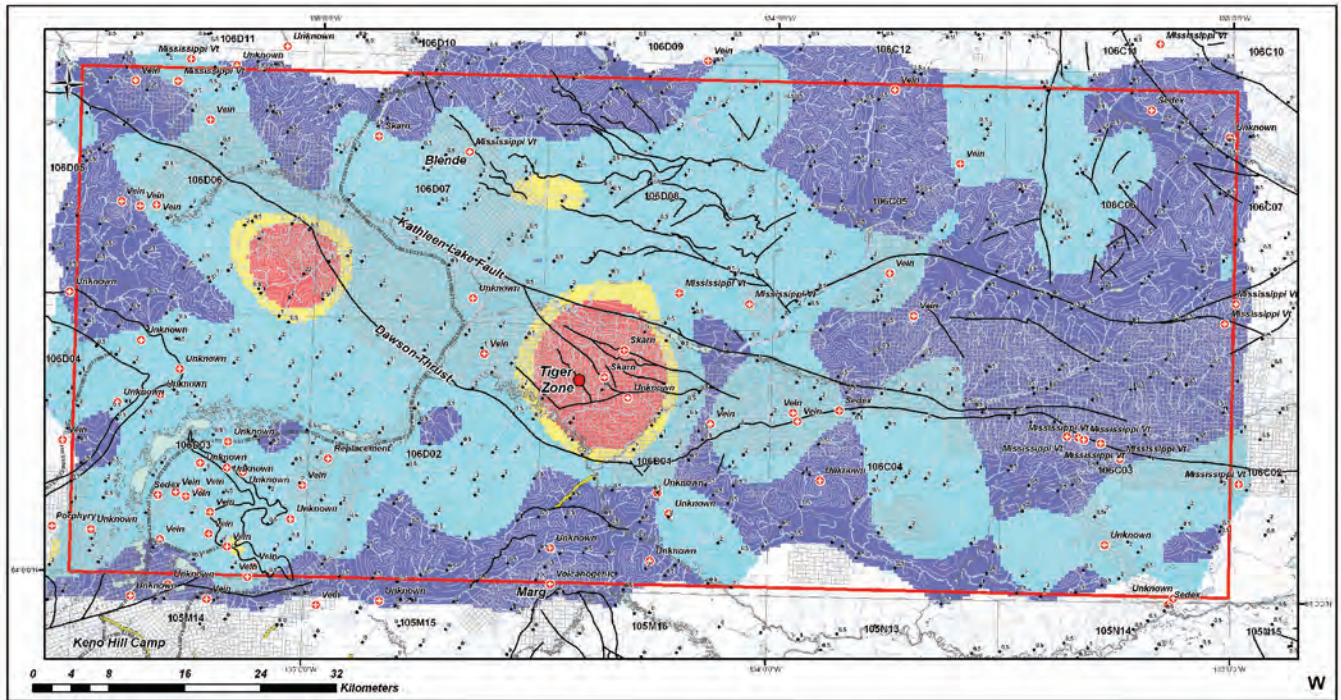


Figure 8. Colour-gradient gridded map of RGS W anomalies in the South Wernecke bedrock project area. Areas in red correspond to 95th percentile (or 2 standard deviations) anomalies in the dataset.

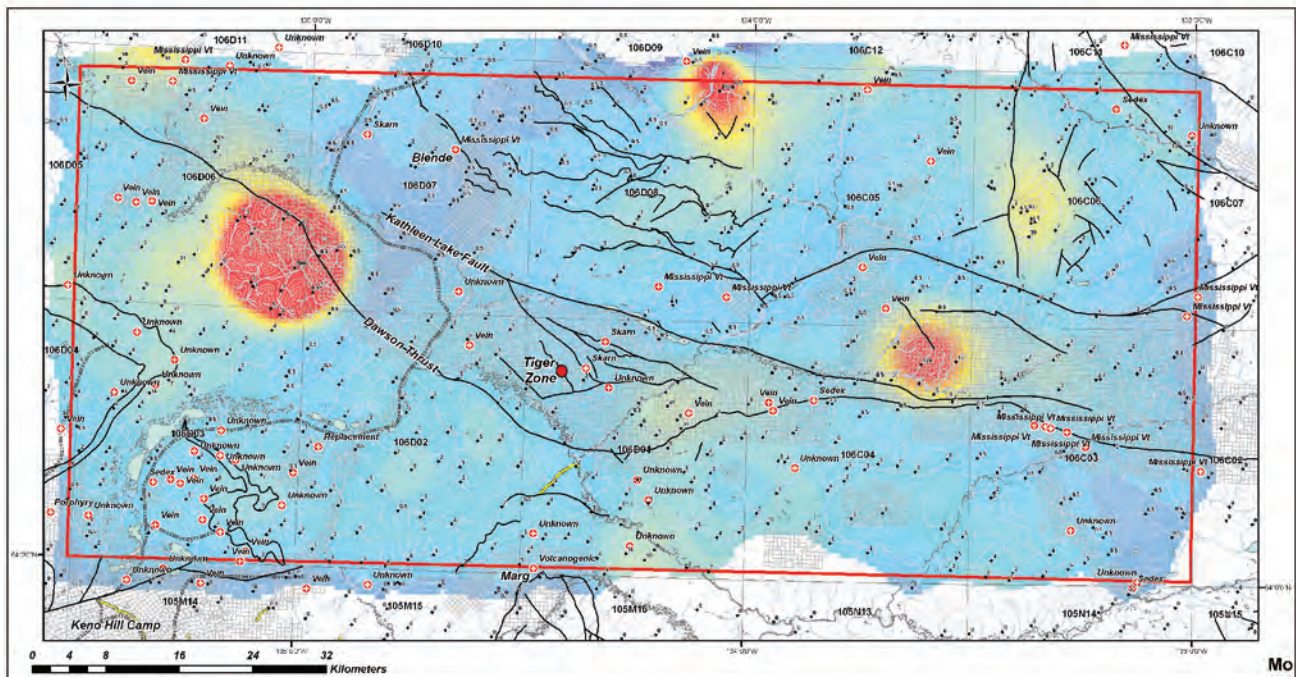


Figure 9. Colour-gradient gridded map of RGS Mo anomalies in the South Wernecke bedrock project area. Areas in red correspond to 95th percentile (or 2 standard deviations) anomalies in the dataset.

SOUTHERN DOMAIN

Rocks comprising the Southern domain include all rocks south of the Dawson Thrust. They are exposed along the ridges north of the Stewart River and through much of the Nadaleen Range, where they sit in the hanging wall of the Dawson Thrust. Units S1 – S6 have in part been correlated with the Neoproterozoic – lower Cambrian Hyland Group (Fritz *et al.*, 1983), and form the structurally lower part of the Dawson Thrust sheet. Units S7 – S9 are in part correlated with the Devonian – Mississippian Earn Group that overlie Hyland Group equivalents. Where primary structures could be identified, stratigraphic up is predominantly to the south. The exact nature (unconformity versus thrust fault) of the contact between the two sedimentary sequences is unclear though relative to units S1-S6, Earn Group equivalent rocks are situated structurally higher in the Dawson Thrust sheet.

Hyland Group (PC_H) equivalents

Unit S1 comprises predominantly grey-brown, blocky weathering, thickly bedded (≥ 1 m) medium to coarse-grained, sandstone and polymictic pebble - cobble conglomerate (Fig. 11a), with minor carbonate and shale. The matrix in coarse-grained sandstones and conglomerates is locally characterized by rusty weathering limonite. Coarse sandstone and conglomerate are locally dolomitic or calcitic, forming massive beds that are separated by intervals of grey-black weathering shales/slates (≤ 1 m; Fig. 11b). Finer grained sandstones are characterized by the presence of detrital white mica.

Unit S2 includes orange-brown, blocky weathering; moderately bedded (≤ 1 m), fine to coarse grained calcareous to dolomitic sandstone with minor polymictic pebble conglomerate (Fig. 11c), and may be equivalent to unit S1 described above. Pebbles include black nodules that may be phosphatic in composition, and rounded quartz and shale chips. Rocks of unit S2 occur most commonly near limestone beds interpreted to belong to the carbonate member of the Hyland Group (PC_{Hc}; Risky Formation?) (Fritz *et al.*, 1991).

Maroon and green, recessive, platy weathering, fine-grained slates comprise unit S3. Based on its distinct colour and stratigraphic position, we correlate S3 with the lower Cambrian Narchilla Formation (C_N; Fig. 11d) of Fritz *et al.* (1991). Unlike the Narchilla Formation at its type locality, traces of *Oldhamia* were not observed in the Mount Mervyn area which may be a consequence of the rocks breaking preferentially along cleavage planes as opposed to bedding.

Unit S4 comprises distinctly green - rusty weathering, fine to medium-grained micaceous sandstones, siltstones and shales (Fig. 11e). Fine-grained sandstone beds are thick (≤ 1.5 m) while intervening shale beds are thin (≤ 10 cm). The unit does not appear in outcrop everywhere, but is abundant in the central part of the Nadaleen Range. Abbott (1990) described a coarse-grained member of the Narchilla Formation, to which we tentatively correlate unit S4.

Lower Paleozoic rocks

Unit S5 is made up of light grey-brown, blocky weathering, fine to coarse-grained limestone. In places, outcrops are made up of boulder size (>0.5 m) limestone clasts that have a brecciated appearance. Clasts are cemented by sparry dolomite and calcite, locally preserving tabulate corals and grains interpreted to be ooids (Figs. 12a,b). The corals are tentatively identified as *Halysites* (E. Turner, personal communication, 2010), implying coral growth on an Ordovician to early Devonian platform. The presence of brecciated clasts indicates disruption and re-deposition of the platform following its formation.

Brown to dark-grey weathering, finely (≤ 0.25 m) laminated siltstones and phyllites (Fig. 12c) comprise unit S6. The package shows marked similarities to green - orange weathering phyllites described in the eastern half of the Nadaleen Range (see Unit C1).

Earn Group (DM_E) equivalents

Units S7 and S8 underlie most of the southern half of map sheet 106C/04. Unit S7 includes grey-black-brown recessive-weathering shale and siltstone of varying carbon content (Fig. 13a), interbedded locally with rare tuffaceous horizons. Siltstone beds are ≤ 0.25 m and commonly characterized by graded, fining upward sequences. Other lithologies include grey chert beds up to 20 cm thick, minor fine-grained sandstone and rare chert-bearing pebble conglomerate. Sandstone beds are typically less than 1 m thick, but locally they are substantially thicker. The thick bedded sandstones were mapped as unit S8.

Sedimentary rocks of units S7 and S8 were assigned to the Devonian – Mississippian Earn Group (DM_E) by Gordey and Makepeace (2001). This correlation is consistent with our field observations. The interpretation will be further corroborated as U-Pb data becomes available for a tuffaceous shale that was sampled in 2010.

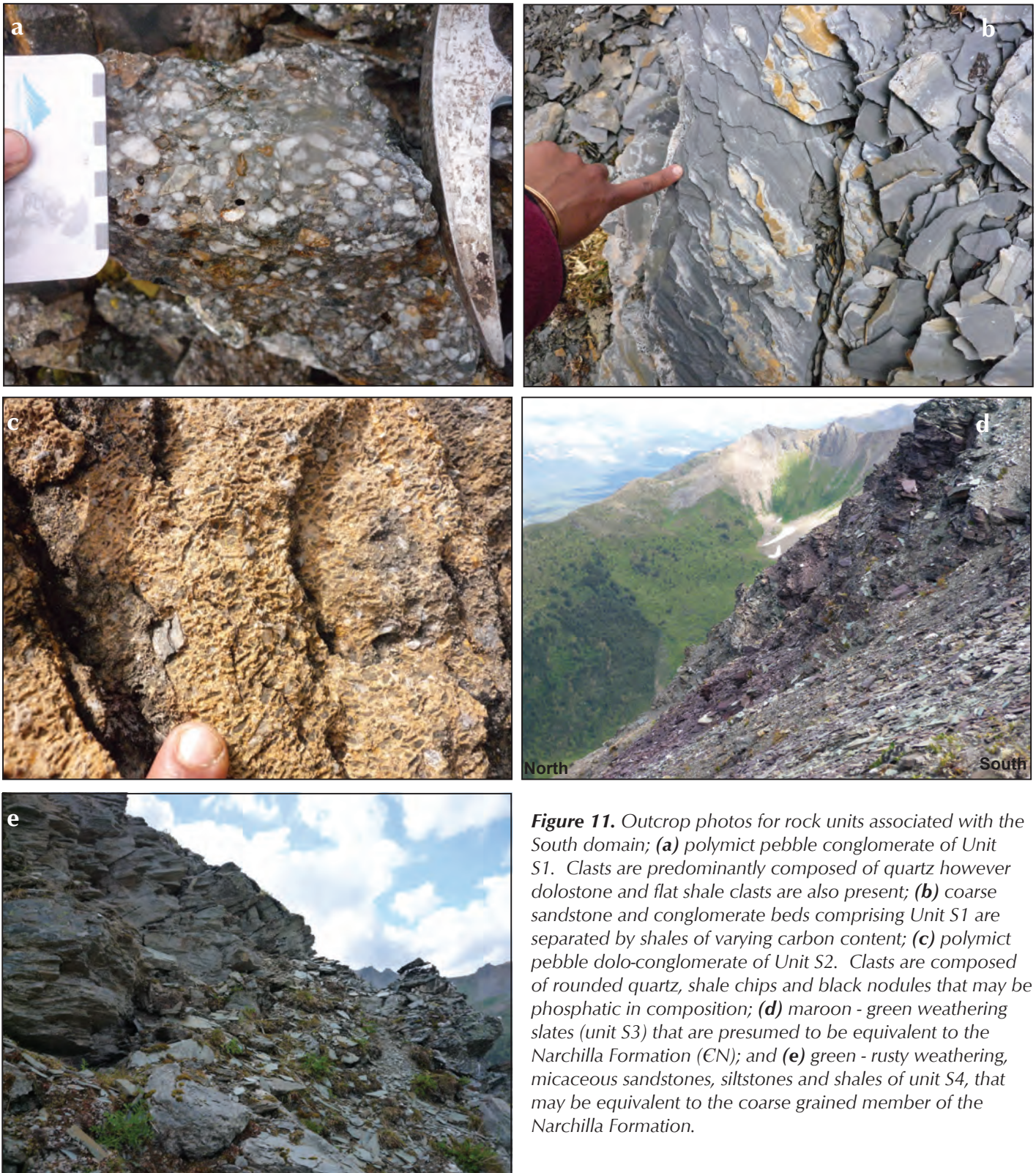


Figure 11. Outcrop photos for rock units associated with the South domain; **(a)** polymict pebble conglomerate of Unit S1. Clasts are predominantly composed of quartz however dolostone and flat shale clasts are also present; **(b)** coarse sandstone and conglomerate beds comprising Unit S1 are separated by shales of varying carbon content; **(c)** polymict pebble dolo-conglomerate of Unit S2. Clasts are composed of rounded quartz, shale chips and black nodules that may be phosphatic in composition; **(d)** maroon - green weathering slates (unit S3) that are presumed to be equivalent to the Narchilla Formation (CN); and **(e)** green - rusty weathering, micaceous sandstones, siltstones and shales of unit S4, that may be equivalent to the coarse grained member of the Narchilla Formation.



Figure 12. Outcrop photos for Paleozoic and potentially equivalent rock units observed throughout in the lower sheet of the South Domain; **(a)** tabulate corals (*Halysites*; E. Turner pers. comm., 2010) weathering out of brecciated limestone clasts of Unit S5; **(b)** ooid like grains weathering out of brecciated limestone clasts of Unit S5; and **(c)** brown-grey-green weathering, laminated siltstones and phyllites of Unit S6.

Triassic rocks

Unit S9 includes dark green - rusty orange/brown, blocky weathering, plagioclase porphyritic intrusions ranging in composition from gabbro to diorite (Fig. 13b). In the southwest corner of the map sheet, the intrusions form tabular bodies that are conformable with bedding in the surrounding sediments. Elsewhere contacts are not as clear and may be discordant with bedding. Mafic rocks of this unit form resistant layers that are visible from kilometres away.

Gordey and Makepeace (2001) included these intrusive rocks with the regionally extensive Triassic Galena Suite. Similar mafic intrusions occur in Lansing Range map area to the south (Roots, 2003), Mount Westman area to the west (Abbott, 1990) and in a west-trending belt from northern Mayo map area (Roots, 1997) to Dawson map area (Green, 1972).

CENTRAL DOMAIN

The Central domain includes rocks north of (*i.e.*, in the footwall of) the Dawson Thrust and south of the Kathleen Lakes Fault. It is divided into four, east-striking units (C1-C4) that are tentatively correlated with Devonian - Mississippian and younger rocks to the west, as described by Abbott (1990).

Unit C1 includes rusty-brown to grey weathering, carbonaceous mudstone, black argillaceous chert with minor siltstones and lesser amounts of light grey weathering limestone (Fig. 14a) that resembles unit C3 described below.

Unit C2 comprises phyllitic lithologies that show marked similarities to unit S3. Phyllitic rocks of this unit are characterized by brilliant orange and green and lesser maroon weathering colours (Fig. 14b), that are interbedded with orange weathering siltstones.

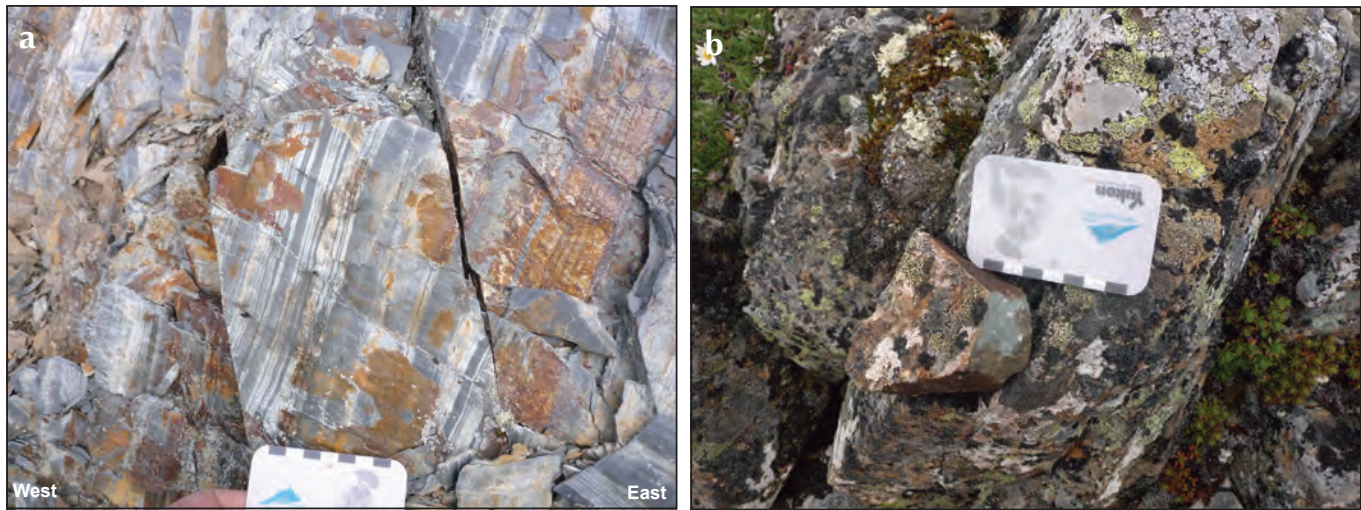


Figure 13. (a) Foliated siltstones and shales of Unit S7 that are presumed equivalent to the Earn Group, (b) plagioclase porphyritic gabbro (Unit S9) that has intruded into, and foliated with siliciclastic rocks of Unit S7.

Light grey weathering, dark grey to black, massive limestone comprises unit C3. Locally this unit is brecciated and cemented with calcite. Conodonts extracted from the limestone are of Permian age (Abbott and Orchard, unpublished data.). Limestone occurrences east of the conodont locality are well bedded (≤ 1 m), characterized by stylolite development and locally preserve lenses of black chert (Fig. 14c). A previously unmapped, apple-green weathering, ultramafic to mafic body comprises unit C4 (Fig. 14d). The rocks, which weather recessively, are pervasively serpentized, talc bearing and magnetic. The southern boundary of the unit is marked by the presence of brilliant orange weathering dolo-calcareous sandstone that is currently mapped as part of unit C2. The ultramafic unit extends eastward into 106C/03 correlating nicely with the east trending aeromagnetic high that is associated with this unit.

NORTHERN DOMAIN

Rocks of the Northern domain comprise an eastward-younging package of siliciclastic and carbonate rocks. The nature of the contact between the Central and North domains across the Kathleen Lakes structure remains unclear (*i.e.*, thrust or strike-slip). Siliciclastic rocks in the region were previously mapped as Hyland Group that is unconformably overlain by platform carbonate rocks of the Cambrian – Devonian Bouvette Formation (Gordey and Makepeace, 2001). Mapping in 2010 revealed that the siliciclastic rocks do not resemble Hyland Group rocks as mapped in the Southern domain. Further mapping and acquisition of geochronological constrains will be required

before a stratigraphic correlation can be proposed with confidence.

Proterozoic rocks

Unit N1 comprises rhythmically bedded, orange weathering limestone/dolostone, grey weathering calcareous sandstone, and shale. Beds are ~ 1 m in thickness, separated by relatively thick (≥ 1 m) shale intervals. Sandstone is fine to medium-grained and characterized by the presence of detrital white mica on bedding planes. Orange dolo- limestone beds preserve fine laminations that may represent algal mats (Fig. 15a).

Green and orange weathering, medium-bedded (≤ 0.5 m), fine-grained siltstones, fine to coarse-grained sandstones and polymict cobble conglomerate constitute unit N2. Pebble lithologies in the conglomerate include dolostone, limestone, shale and dull grey chert (Fig. 15b). Varying concentrations of dolomitic cement are present in beds of all grain size. Graded bedding in conglomerates indicate locally overturned beds that young to the northwest. The contact between N2 and overlying unit N3 is gradational over 2-5 metres.

Unit N3 comprises red-brown and locally green weathering, medium to thick-bedded (≥ 1 m; Fig. 15c), fine to medium-grained sandstone, siltstone and lesser shale. Primary sedimentary structures are weakly preserved in coarser grained beds and locally indicate tops to the west-northwest. The distribution of unit N3 in the map area suggests a syncline (cored by the overlying unit N4; Fig. 10); although only west-northwest-younging beds were



Figure 14. Outcrop photos for Permian and potentially equivalent rock units observed throughout the Central domain; **(a)** rusty brown - grey green weathering carbonaceous mudstone (unit C1) surrounded by light grey weathering limestone that looks texturally similar to limestone of Unit C3; **(b)** outcrops of green - brilliant orange and lesser maroon weathering phyllites that show some similarities to unit S3, but are currently classified as Unit C2 and may be more closely related to Unit S9; **(c)** well bedded limestone of Unit C3 where preservation of black chert lenses was noted and contacts between bedding planes marked by stylolite development; and **(d)** a typical 'outcrop' of the previously unmapped, brilliant apple-green weathering ultramafic - mafic Unit C4.

observed in the field, the geometry, if correct, implies overall eastward younging of the unit.

Unit N4 includes dark grey to grey-white weathering limestone with lenses of finely laminated black chert (Fig. 15d). Bedding is poorly defined but generally less than 0.5 m thick. Chert lenses are 5-10 cm thick and characterized by fine laminations that give a stromatolitic/algal appearance, a feature of chert associated with Proterozoic limestones elsewhere (E. Turner, pers. comm. 2010). Massive (>2 m) chert with siliclastic clasts occurs locally and may represent a debris flow deposit.

Rocks of unknown age and correlation

Beige to white to orange weathering, massive to chaotic limestone-dolostone constitutes much of unit N5. Rocks are brecciated in places and made up of vuggy limestone boulders locally with ooids up to 0.5 cm in diameter (Fig. 15e). Vugs are filled with calcite and/or quartz.

Elsewhere, more dolomitic lithologies are well bedded (~1 m thick) and preserve cryptalgal laminations. Locally, rocks are characterized by networks of quartz veins (Fig. 15f).

Unit N6 comprises pink to rose coloured, fine-grained siltstone that is finely laminated with beige dolostone and minor limestone (Fig. 16a). In one locality rosy pink weathering rocks grade eastward into texturally identical green-weathering siltstone laminated with beige dolostone and minor limestone. Unit N6 is similar to Precambrian unit 1 of Morrow (1999).

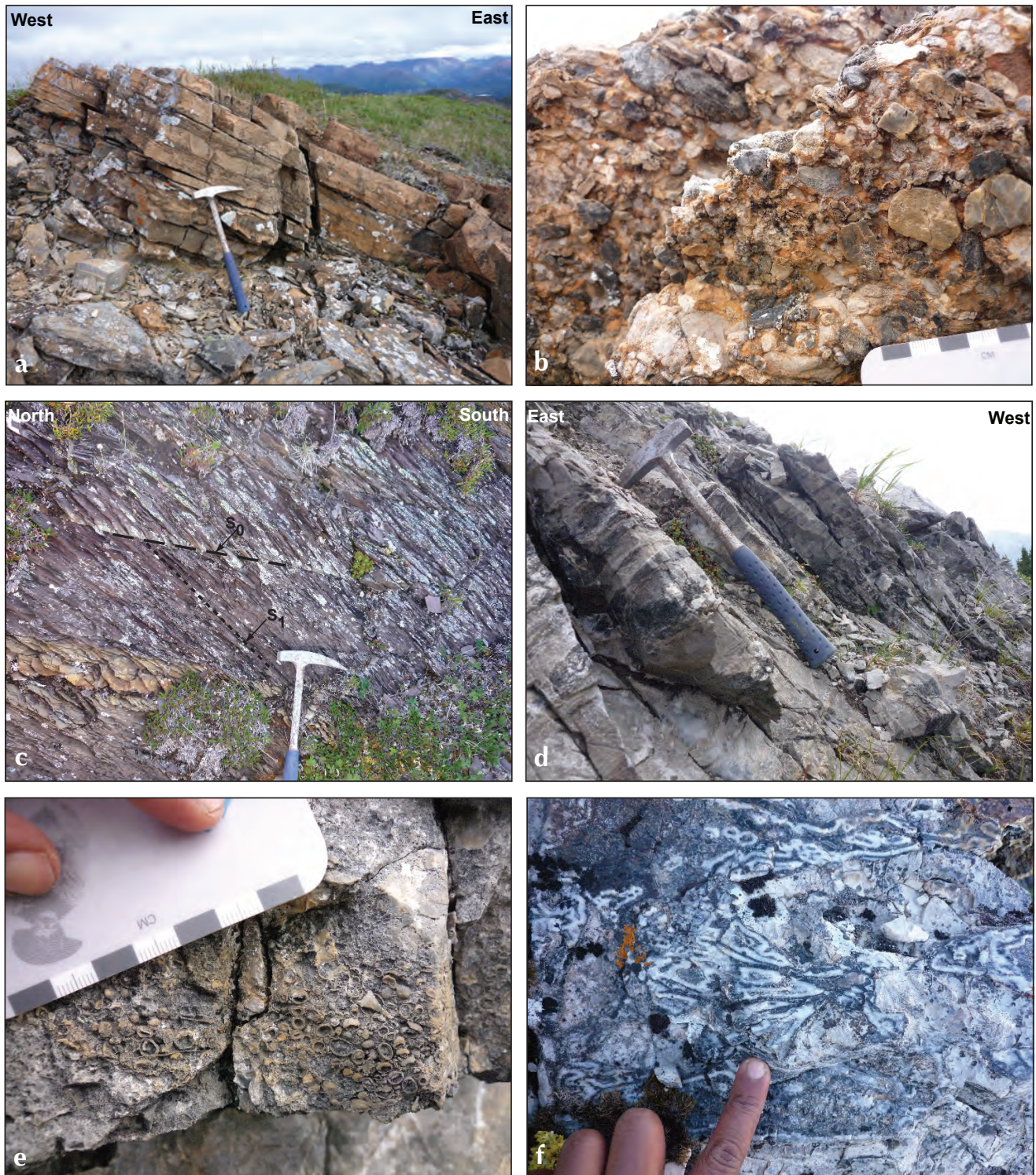


Figure 15. Outcrop photos for rocks comprising the North domain; **(a)** orange dolo- limestone beds of Unit N1. Fine laminations may represent algal mats; **(b)** green and orange weathering polymictic cobble conglomerate of Unit N2. Pebble compositions include limestone, dolostone, shale and dull grey chert; **(c)** red-brown siltstones and sandstones of Unit N3. Note the well developed cleavage (S_1) and its discordance with bedding (S_0); **(d)** unit N4 bedded limestones and associated black chert of potential Proterozoic age; **(e)** ooid grains weathering out of brecciated limestone blocks of 'chaotic' of unit N5; and **(f)** epithermal like quartz textures observed locally within seemingly massive and chaotic limestone of unit N5.

Rusty brown weathering, medium-grained, laminated to finely bedded (≤ 20 cm) sandstone interbedded with siltstone (≥ 1 m thickness) characterize Unit N7 (Fig. 16b). Centimeter-scale graded beds indicate younging to the southeast. Rocks of this unit are strikingly similar to the siliciclastic component of unit N1 described above. Correlation between the two units will depend on geochronological constraints as they become available. Bedding in Unit N7 is discordant with overlying limestone of unit N8 (see below), suggesting the contact between the two units is either faulted or represents an angular unconformity.

Bouvette Formation (CD_B) equivalents:

Unit N8 is well to cryptically bedded, light grey weathering limestone. Beds are less than 1.5 m thick with preservation of black chert locally. In places, limestone beds appear to be graded storm beds (*i.e.*, tempestites?) and/or pelloidal grainstones. Rare fossils include crinoid fragments and gastropods (Fig. 16c). Locally, zones of extensive brecciation up to ~ 100 m thick were observed. Limestone clasts within the brecciated intervals are angular and cemented with sparry calcite and dolomite. While N8 structurally overlies N7, an angular discordance between bedding in the two units suggests that a fault contact or an angular unconformity separates them. The unit underlies a significant area in the eastern part of the Northern Domain and appears also to extend south, across the Kathleen Lakes fault. Conodont samples have been collected from all localities and will provide constraints with which stratigraphic correlations can be made with confidence.

Green to rusty brown weathering, fine to medium-grained, well bedded (≤ 1 m) quartz sandstone and siltstone of unit N9 overlie limestone of unit N8. The base of the unit is characterized by a medium to coarse-grained, orange weathering, fossiliferous sandstone (~ 1 m thickness) with crinoid and brachiopod fragments (Fig. 16d). Higher up-section, grey-green siltstone beds are blocky-weathering and have been bioturbated (Fig. 16e), in places preserving pyrite filled burrows. Coarser sands preserve climbing ripples (Fig. 16f) and graded bedding that indicates younging to the southeast.

Unit N10 comprises both well bedded (≤ 1 m thickness) and locally brecciated, light to dark grey weathering limestone (Fig. 17a). The base of the unit is characterized by the presence of crinoid fragments. In outcrops that comprise brecciated limestone boulders, isolated boulders preserve tabulate (*Favocites?*) \pm solitary corals (*Rugosian*; Figs. 17b,c) and possibly stromatoporoids (Fig. 17d).

Preservation of sponges and horn corals suggests this unit is Ordovician – Devonian in age.

Based on field observations made to date, Units N8 to N10 are interpreted to be part of the Bouvette Formation (Morrow, 1999). If this correlation is correct, the rocks represent platform carbonates deposited on the edge of the Selwyn basin, and are time-equivalents to clastic rocks of the Gull Lake and Road River groups to the south of the study area.

STRUCTURAL GEOLOGY

Structural elements preserved in the map area vary within and between domains, and are not yet well-understood. Evidence for multiple generations of fabric development are locally recognized in outcrop, however correlation of fabrics noted in units of different age and structural level have not yet been established. References to fabrics S_1 , S_2 , etc. are used to describe local overprinting relationships and are not to be applied on the regional scale at this time. In spite of unresolved details, fabrics descriptions and general observations about structural vergence are presented below.

SOUTHERN DOMAIN:

Rocks of the Southern domain make up the hanging wall of the Dawson Thrust. Rocks that occupy the thrust stack are divided into two packages (Fig. 10). The oldest of the sedimentary packages is situated immediately above the Dawson Thrust and includes units S1-S6. Structurally above them is a younger package (S7 to S9) that is in direct contact with the oldest stratigraphic unit (*i.e.*, S1). Based on the inferred correlation of S7 and S8 with Earn Group rocks, the juxtaposition of units S1 and S7 suggests either an angular unconformity or a faulted contact.

Immediately above the Dawson Thrust, older rock units in the structurally lower part of the thrust stack are deformed into north-verging folds and faults (Figs. 18a-c). Where bedding (S_0) and primary sedimentary structures have been identified, stratigraphic 'up' is most commonly to the south. Isolated occurrences for overturned, northward younging beds have also been documented though their occurrence is relatively minor. The main penetrative foliation (S_1) is best developed in less competent lithologies (*i.e.*, shale), and is shallowly to steeply south-dipping. Fold hinges plunge shallowly to moderately to the east and west. Variations in plunge imply more than one phase of folding, although in most outcrops only one penetrative foliation is preserved.



Figure 16. (a) Distinctly rosy pink, finely laminated siltstones interbedded with beige dolostone and minor limestone of Unit N6; (b) laminated – finely bedded sandstones that are interbedded with siltstones and together form Unit N7; (c) though sparse, gastropod fossils may be found in limestone beds of Unit N8; (d) a fossil hash in sandstone at the base of Unit N9 preserving gastropod and crinoid fragments here photographed through a x16 hand lens; (e) pyritized burrows preserved in a siltstone bed (Unit N9); and (f) climbing ripples preserved in a sandstone bed of Unit N9.

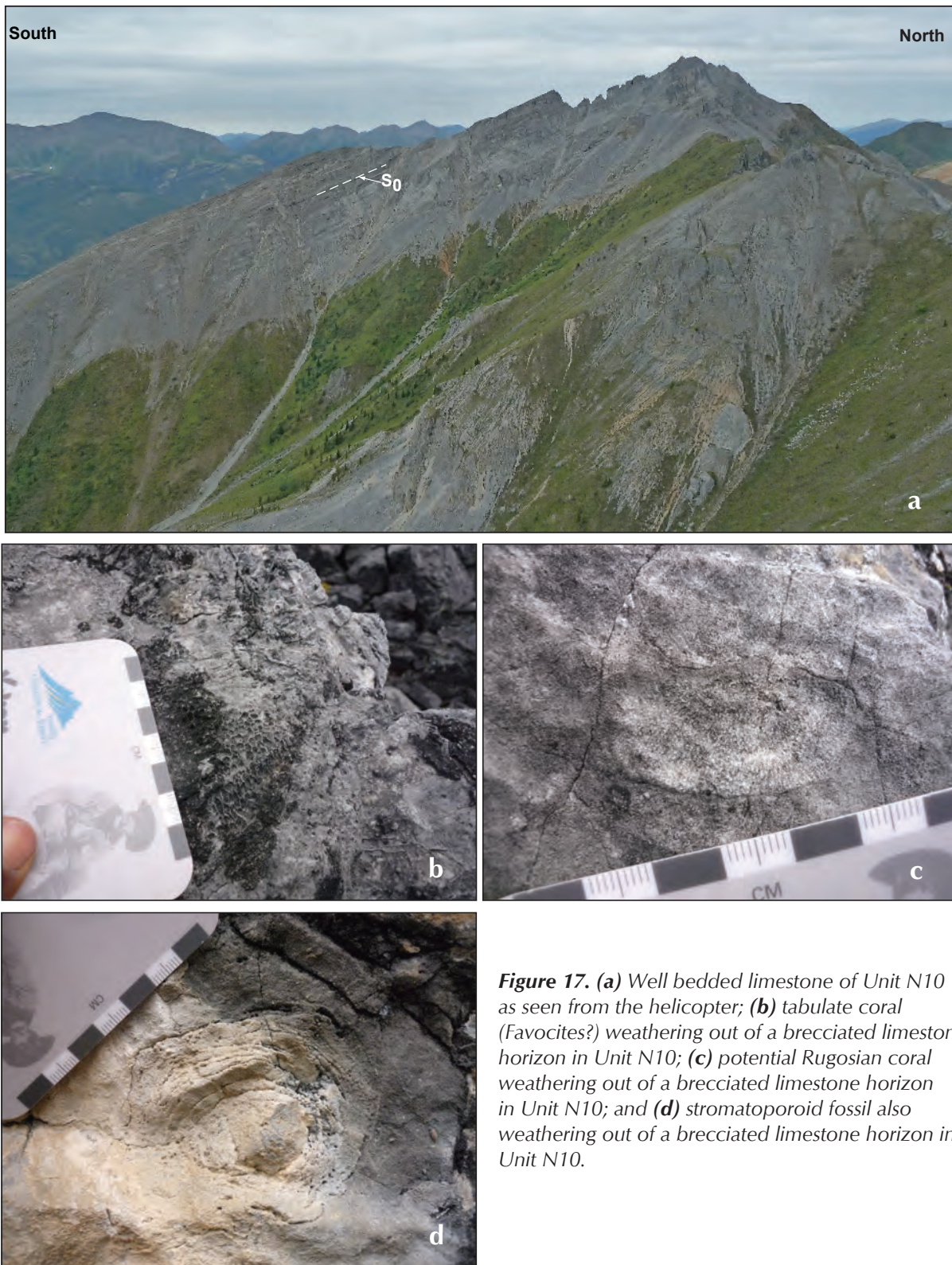


Figure 17. (a) Well bedded limestone of Unit N10 as seen from the helicopter; (b) tabulate coral (*Favocites?*) weathering out of a brecciated limestone horizon in Unit N10; (c) potential *Rugosian* coral weathering out of a brecciated limestone horizon in Unit N10; and (d) stromatoporoid fossil also weathering out of a brecciated limestone horizon in Unit N10.

At higher structural levels, immediately south of the contact between units S1 and S7, beds within Earn Group rocks are predominantly east-striking and moderately to steeply south dipping. Primary sedimentary structures indicate southward younging throughout much of unit S7 though minor variations have also been documented (*i.e.*, east- and southeastward younging; Fig. 18d). The main (S_1 ?) foliation at this locality is similar in orientation to that observed in the underlying units (S1 – S6), dipping moderately to steeply to the south. Locally in outcrop, the main (S_1) foliation surface is characterized by the development of a crenulation (S_2) resulting in a shallowly east – southeast plunging intersection lineation (L_2 ; Fig. 18d).

In the southwest corner of the Mount Mervyn map sheet, at even higher structural levels of the Southern domain, beds (S_0) in rocks of the Earn Group (S7 and S8) dip moderately to the north. Graded beds generally indicate northward younging, with evidence also for overturned, south-facing beds implying the presence of tight folds (F_1 ?). Overprinting these rocks is a variably north-dipping penetrative foliation (designated S_2), that is best developed in shale layers and interpreted to be axial planar to large-scale, upright, open (F_2) folds that have refolded the earlier F_1 folds.

Unlike the siliciclastic rocks they intrude, tabular Triassic mafic bodies preserve evidence for only one phase of deformation. They define upright, open folds that plunge gently to the east (Fig. 18e). It is possible that these folds are correlative with a second-generation synform that deforms unit S7 (described above), as their axial surfaces are roughly parallel.

CENTRAL DOMAIN

Green, L. (1972) described rocks in the footwall of the Dawson Thrust as complexly deformed (Fig. 19a). However, the map pattern defined by units in the Central domain does not appear complicated. Similar to the fabrics observed in the immediate hanging wall of the Dawson Thrust fault, bedding and a penetrative bedding-parallel foliation are folded and thrust-imbricated to the north. Both fabrics (bedding and foliation) define asymmetric folds with long shallowly south-dipping limbs and short steeply north-dipping limbs. Hinges plunge shallowly to moderately east and west. Southward younging of beds indicate an upward-facing stratigraphic pile as is also documented in the immediate hanging wall of the overriding thrust (Southern domain).

Variations in fold plunges and the fact that the folds deform a pre-existing foliation suggest the area was subject to more than one phase of deformation. Curved fold plunges (Fig. 19b) suggest the main north-verging folds have been refolded; however, it is possible that the curvature is simply a result of non-coaxial strain, which may be a possibility given the setting of the Central Domain between two major crustal-scale faults.

NORTHERN DOMAIN

Rocks in the Northern domain are situated north of the Kathleen Lakes fault, the kinematics of which is currently unknown. Relative to the domains described above, rocks of the Northern domain are weakly deformed. Bedding orientations are variable though dominantly north-striking and moderately east dipping. Although stratigraphic tops are difficult to decipher in outcrop, the package as a whole youngs eastward.

In the western part of the Northern domain, overturned beds (younging to the northwest) have been identified in units N2 and N3 at two localities east of unit N4. The presence of overturned beds coupled with the symmetrical distribution of N2 and N3 implies the presence of a roughly north trending syncline that is cored by limestone unit N4 (Fig. 10).

Foliation development is restricted to finer grained rocks, and is observed in only three units: the fine layers within units N2, N3 and locally in N6 (Figs. 15c and 16a). Everywhere that it is observed, the foliation is east-striking and dips shallowly to moderately southward. The foliation strikes roughly parallel to the postulated east-trending open folds described above, suggesting a possible correlation.

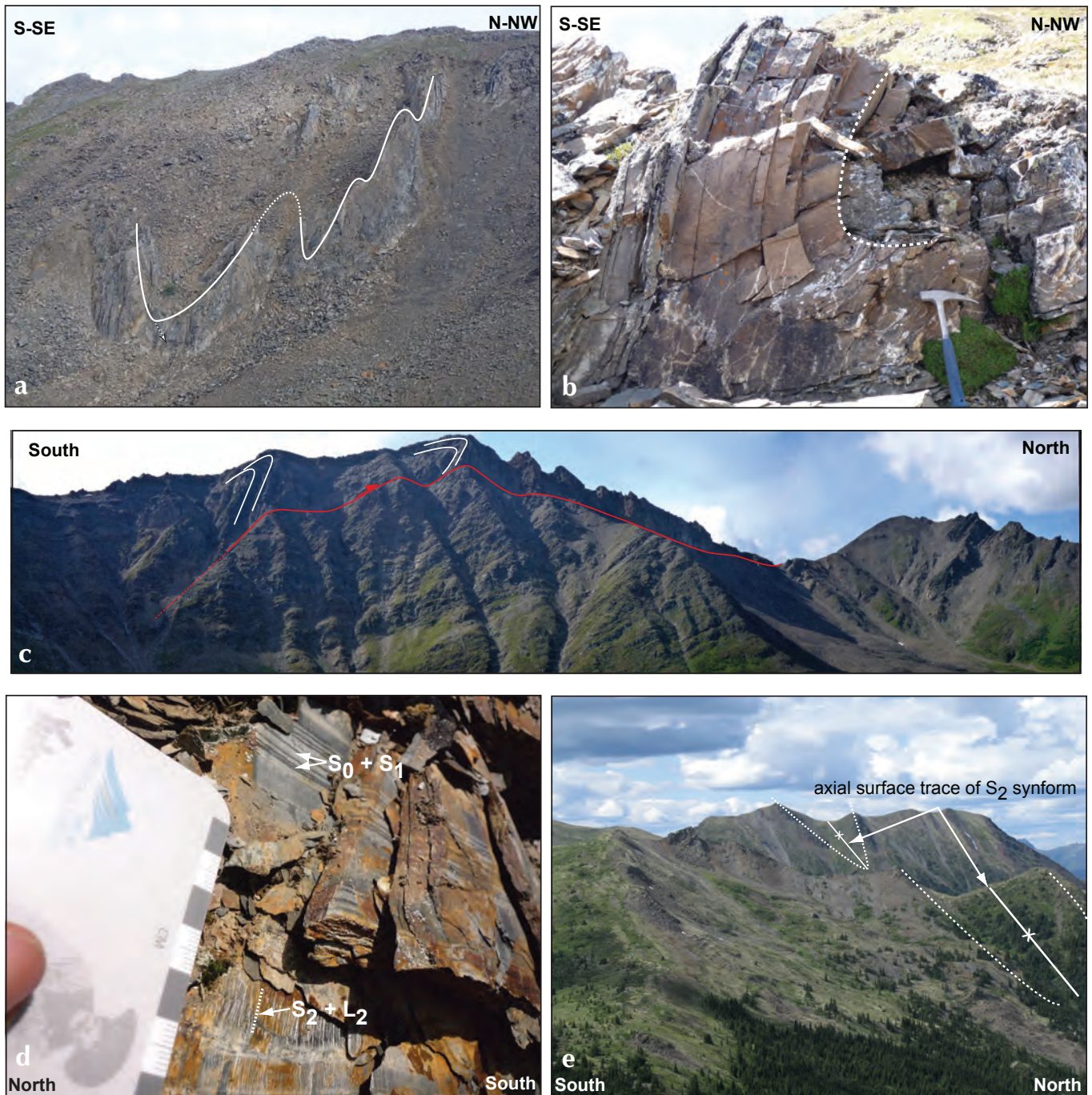


Figure 18. Photographs illustrating the complex structures observed throughout the South domain; **(a)** northwest verging fold exposed on the southeast side of a mountain in southwestern part of the Nadaleen Range. The fold is developed in Hyland Group equivalent strata of unit S_1 ; **(b)** outcrop scale synform developed in unit S_1 ; **(c)** in addition to intense folding, siliclastic and carbonate rocks in the 'lower' sheet of the South domain have also been thrust northward on the kilometer scale (photo is ~ 500m in width); **(d)** outcrop of Unit S_7 siliclastic rocks highlighting the relationships between bedding (S_0), cleavage (S_1 and/or S_2) and intersection lineations (L_2) between crenulations and the penetrative cleavage; and **(e)** view to the west illustrating the landscape and resistant weathering nature of Unit S_9 with respect to surrounding siliclastic rocks. Also highlighted in the photograph is an S_2 synform that can be visibly traced out by following tabular gabbroic bodies from a distance.



Figure 19. Photographs illustrating fold development within the Central domain; (a) north verging fold developed in Paleozoic limestone of unit C3. For a reference scale, note the author sitting on the hinge of the antiform, and (b) an example of folding on the scale of a 'door-stop' sized sample in strata this is currently correlated with unit S1. Note bedding in this sample appears 'twisted'.

MOUNT MERVYN 2010 REGIONAL SOIL GEOCHEMISTRY SURVEY

In 2010, a regional ridge and spur soil sampling campaign was carried out in parallel with the bedrock mapping of Mount Mervyn map area (106C/04). Reasons for undertaking the survey include i) integration of soil geochemical data with bedrock information collected at the same site, ii) to examine whether a regional scale soil survey might highlight areas of anomalous metal content that would not otherwise be identified by bedrock mapping, and, iii) to assess whether anomalous soil values might relate to existing anomalies identified within the RGS datasets. Results of the survey are presented below, following the description of bedrock geology in the Mount Mervyn area.

METHODOLOGY

Ridge and spur soil samples (C- horizon) were collected using a soil auger and data captured using the 'Dirtbagger' database of Ground Truth Exploration. Data recorded for each soil sample in the pilot study included station number and associated UTM co-ordinates, sampling method

(i.e., auger vs. matic), soil colour, position on slope, sampling depth, soil quality, soil horizon, tree cover, ground cover, other related notes, and photos of each sample site. Including duplicates, a total of 118 ca. 2.2 kg soil samples were collected at ca. 500 m spacing (Fig. 20). Locations broadly correspond to bedrock station localities. Samples were processed and analyzed by ACME Laboratories, using analytical package 1DX2 (aqua regia digestion of a 15 g sample) and analysed by ICP-MS for 36 elements including Hg. We present results for Au, As, and Ni below. The full geochemical dataset is found in Appendix 1.

RESULTS

The resulting soil geochemistry for Au, As and Ni are graphically presented in Figures 21 – 23 respectively. Interval ranges are based on and defined by the natural breaks in the data sets for each element, and represented as graduated symbols. For ease of comparing the new soil geochemistry with both existing surface geochemical data and bedrock geology, symbols are superimposed on the colour-gradient RGS data and new bedrock geology data.

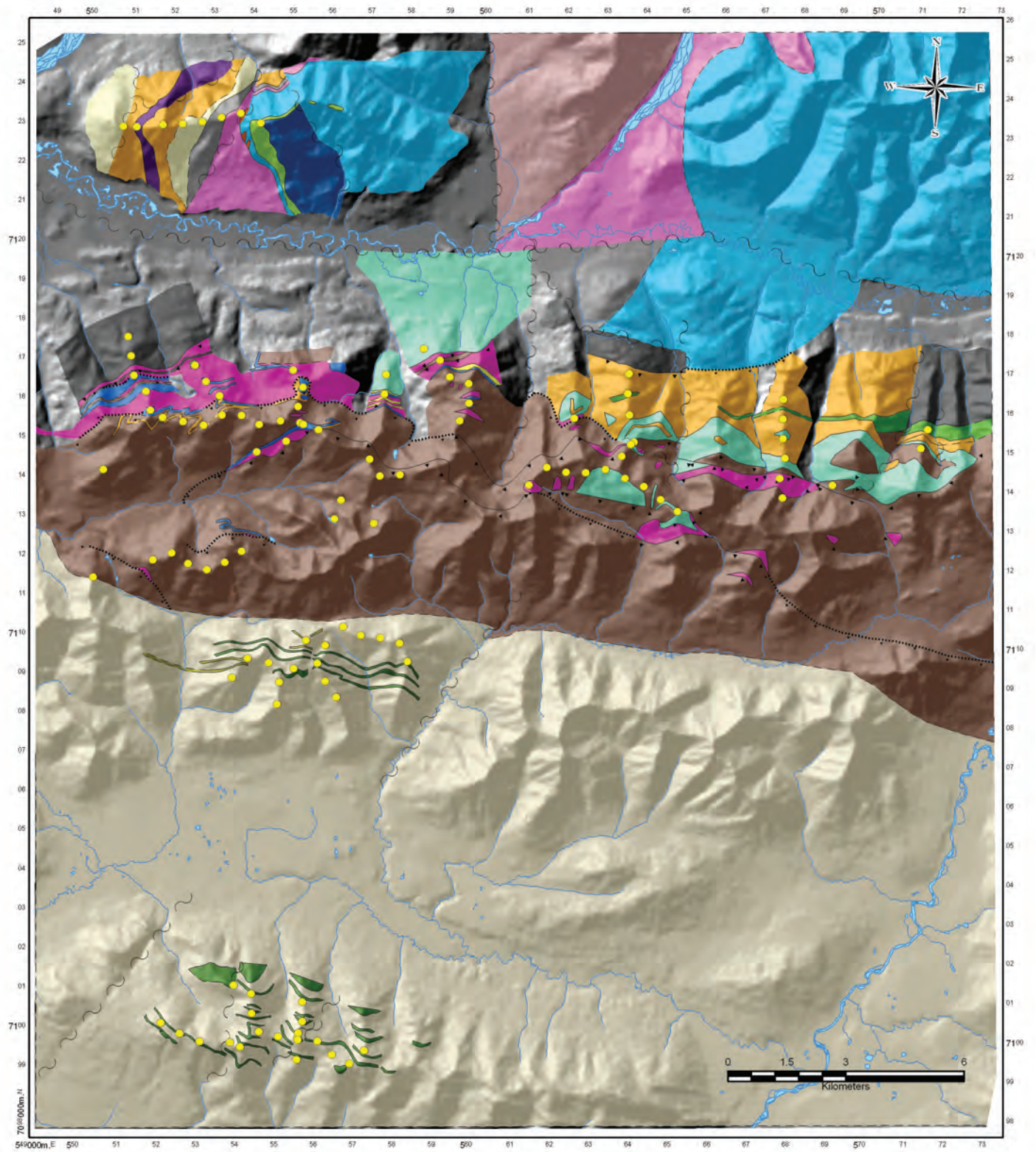


Figure 20. Soil sampling localities superimposed on preliminary bedrock map for the 1:50K Mount Mervyn map sheet (106C/04). Legend as for Figure 10.

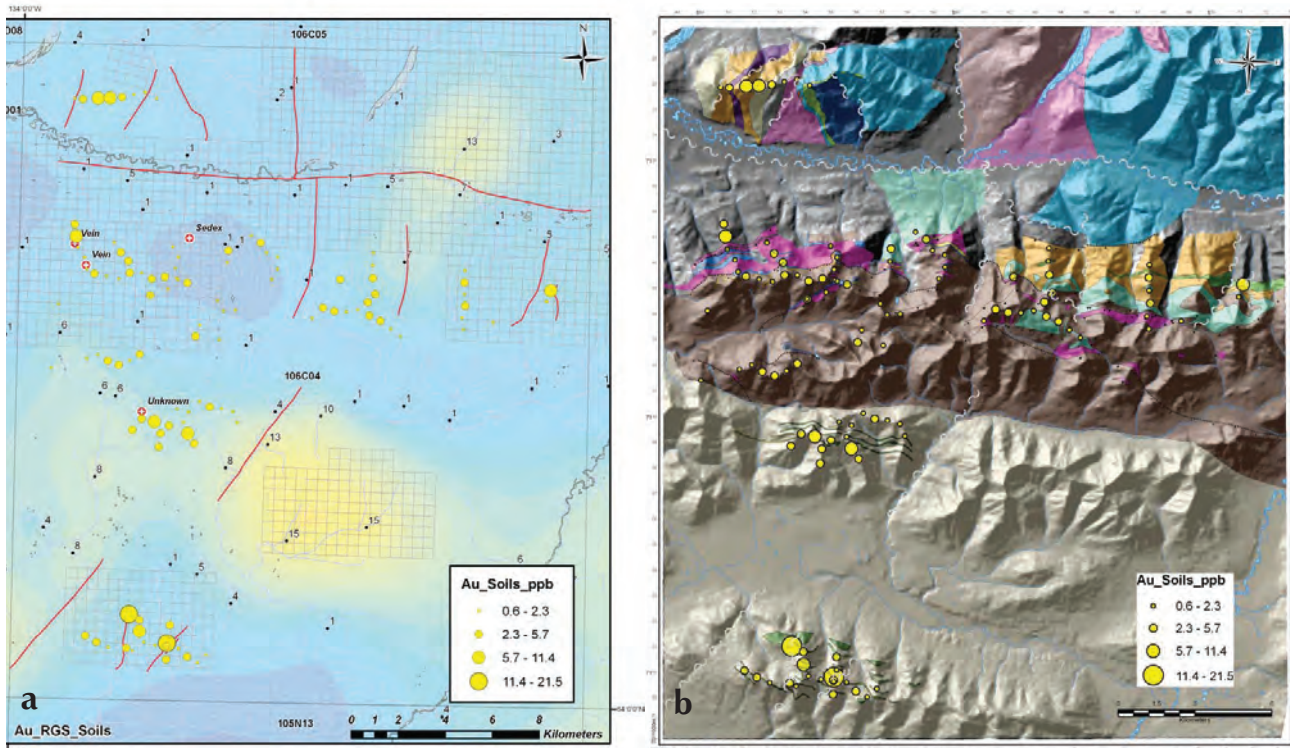


Figure 21. (a) Graduated symbols of Au-in-soils (natural breaks interval classification) superimposed on colour-gradient gridded map of RGS Au anomalies in the Mt Mervyn map sheet area. Values of Au-in-RGS marked (ppb). Yukon MINFILE occurrences marked. (b) Graduated symbols of Au-in-soils superimposed on new bedrock geology data for Mt Mervyn map sheet area.

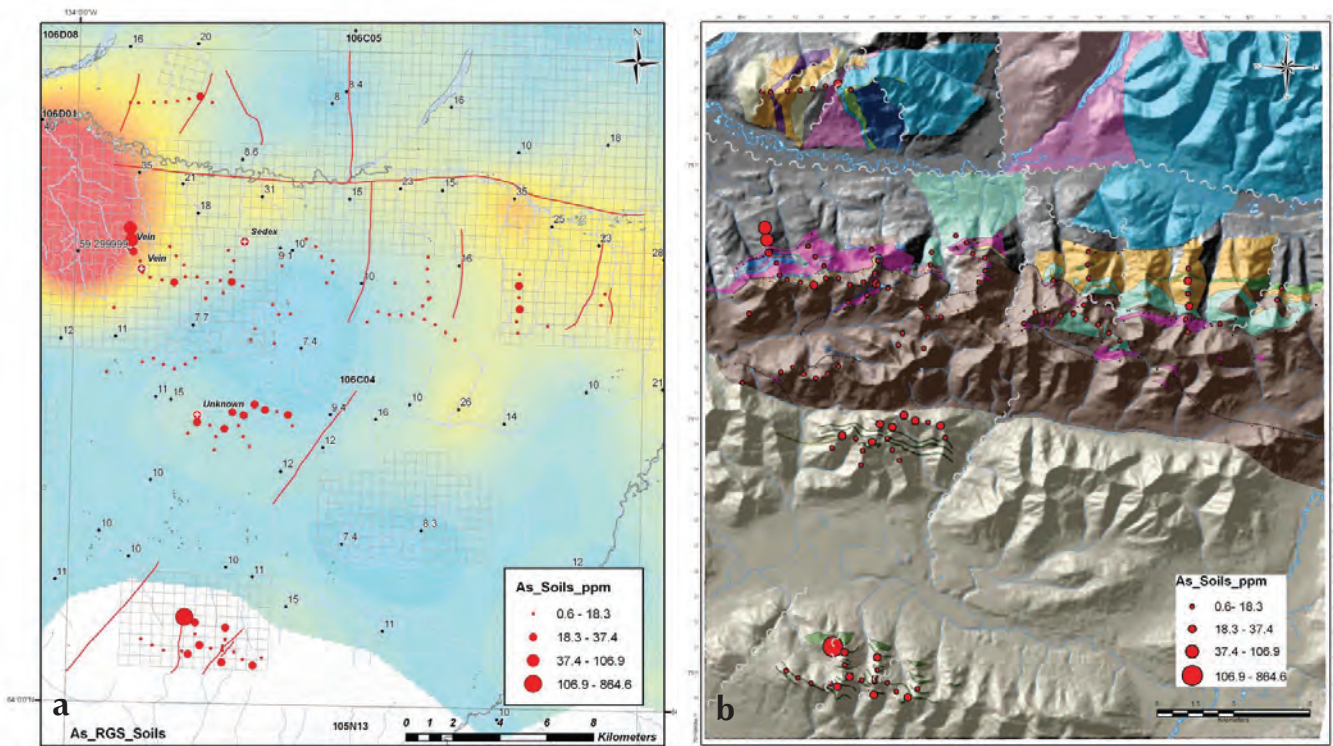


Figure 22. Graduated symbols of As-in-soils (natural breaks interval classification); (a) superimposed on colour-gradient gridded map of RGS As anomalies in the Mt Mervyn map sheet area. Values of As-in-RGS marked (ppm). Yukon MINFILE occurrences marked, and (b) superimposed on new bedrock geology data for Mt Mervyn map sheet area.

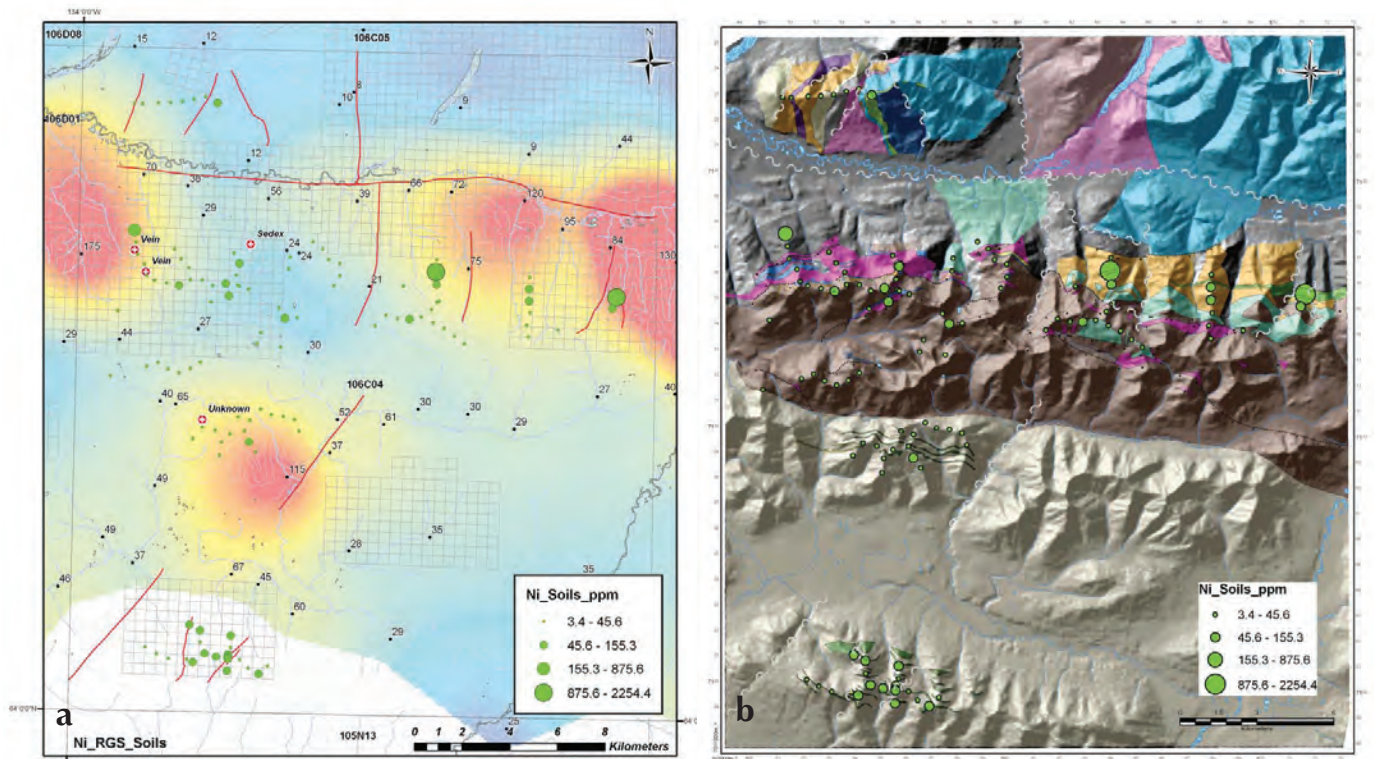


Figure 23. Graduated symbols of Ni-in-soils (natural breaks interval classification); (a) superimposed on colour-gradient gridded map of RGS Ni anomalies in the Mt Mervyn map sheet area. Values of Ni-in-RGS marked (ppm). Yukon MINFILE occurrences marked, and (b) graduated symbols of Ni-in-soils superimposed on new bedrock geology data for Mt Mervyn map sheet area.

Integration of the three datasets highlights:

1. Elevated Au-in-soil values (Fig. 21) are present in at least two of the structural domains defined above, including three areas with more than one anomalous soil sample. RGS values from watersheds draining the three anomalous soil regions are not elevated in Au (Fig. 21a). Bedrock information for sites with elevated gold-in-soil values coincide with the presence of north and north-northeast-trending late fault zones (Fig. 21b). A single anomalous gold-in-soil value is also identified adjacent to a N-trending fault that cuts unit C4 (mafic to ultramafic body) in the Central domain.
2. Anomalous As-in-soil values (Fig. 22) correspond with elevated Au in the southwestern corner of the Mount Mervyn map area. Elevated As values show a strong spatial correlation with high As in the RGS data in the Central domain of Mount Mervyn, which corresponds to known occurrences of polymetallic veins (106C087; Fig. 22).
3. Anomalous Ni-in-soil values (Fig. 23) correlate directly with the occurrence of the mafic-ultramafic layers (unit C4) in the Central domain, and are substantiated by anomalous Ni in the RGS data (Fig. 23).

SUMMARY AND CONCLUSIONS

Regional ridge and spur soil geochemical data are useful for establishing the baseline geochemical signature of underlying bedrock and is a useful tool to aid in identifying regions of enriched metals that may be overlooked by the RGS database.

With respect to the underlying bedrock geology, field work has highlighted lithological complexities that will require new geochronological data before they can be correlated with confidence to surrounding Proterozoic and Paleozoic units. The division of the study area into three structural domains bounded by the Kathleen Lakes and Dawson Thrust faults highlights the different lithological packages and deformation styles across the study area. New geochronologic data will help to bracket the timing of fabrics in the region and enhance existing tectonic interpretations.

ACKNOWLEDGEMENTS

Special thanks to my field assistant Nicolai Goepfel for his much appreciated assistance, unyielding enthusiasm for the mountains and willingness to take charge of the soil sampling aspect of the project. To Isaac Fage of Ground Truth Exploration, for teaching Nic the ABC's of soil sampling. Much gratitude is extended to Mike Burke and Venessa Bennett for their encouragement and support in acquiring some of the data presented here. To Archer, Cathro crews out of the McQuesten and Rau camps, a great deal of appreciation is extended for their support with fly camp moves and for the invitation to participate in Harry Cook's carbonate workshop. Extra special thanks also to Craig McMillian, our Hugues 500 pilot with Fireweed, for gracing us with his talents of flying us safely through and over the hills. Thanks to Don Murphy for the time spent in review of the manuscript and to Carolyn Relf for her editing efforts. Last but not least, this project would not be possible without the support of the YGS. A special mention of thanks is extended to Laurie Fahr, Bailey Staffen, Karen MacFarlane and the YGS technical team as a whole for being so willing and wanting to work together as a team.

REFERENCES

- Abbott, G., 1990. Preliminary results of the stratigraphy and structure of the Mt. Westman map area, central Yukon. *In: Current Research, Part E, Geological Survey of Canada, Paper 90-1E, P. 15-22, 1990.*
- Abbott, G., 1997. Geology of the upper Hart River area eastern Ogilvie Mountains, Yukon Territory (116A/10, 11). Exploration and Geological Services Division, Yukon Region, Indian and Northern Affairs Canada Bulletin 9, 92 p.
- Blusson, S., 1974. Bedrock geology of the Nadaleen Range map area (NTS 106C), central Yukon. Geological Survey of Canada, Open File 1974.
- Fritz, W.H., Narbonne, G.M. and Gordey, S.P., 1983. Strata and trace fossils near the Precambrian-Cambrian boundary, Mackenzie, Sewlyn and Wernecke mountains, Yukon and Northwest Territories; *In: Current Research, Part B, Geological Survey of Canada, Paper 83-1B, p. 365-375.*
- Fritz, W.H., Cecile, M.P., Norford, B.S., Morrow, D. and Geldsetzer, H.H.J., 1991. Cambrian to Middle Devonian assemblages. *In: Geology of the Cordilleran Orogen in Canada, H. Gabrielse and C.J. Yorath (eds.), Geological Survey of Canada, Geology of Canada, no. 4, p 151-218.*
- Gabrielse, H., 1967. Tectonic evolution of the northern Canadian Cordillera. *Canadian Journal of Earth Sciences, vol. 4, pp. 271-298.*
- Green, L.H., 1972. Geology of Nash Creek, Larsen Creek, and Dawson map-areas, Yukon Territory (106D, 116A, 116B, and 116C (E^{1/2})) Operation Ogilvie. Geological Survey of Canada, Memoir 364, 157 p.
- Green, L.H. and Roddick, J.A., 1962. Geology, Nash Creek, Yukon Territory. Geological Survey of Canada, Preliminary Map 15-1962.
- Gordey, S.P. and Anderson, R.G., 1993. Evolution of the Northern Cordilleran Miogeocline, Nahanni Map Area (105I), Yukon and Northwest Territories. Geological Survey of Canada, Memoire 428, 214 p.
- Gordey, S.P. and Makepeace, A.J., 2001. Bedrock Geology, Yukon Territory; Geological Survey of Canada, Open File 3754, Exploration & Geological Services Division, Yukon Indian and Northern Affairs Canada, Open File 2001-1, scale 1:1 000 000.
- Héon, D. (compiler), 2003. Yukon Regional Geochemical Database 2003 – Stream sediment analyses. Exploration and Geological Services Division, Yukon Region, Indian and Northern Affairs Canada.
- Macdonald, F.A., Smith, E.F. Strauss, J.V., Cox, G.M., Halverson, G.P. and Roots, C.F., 2011, this volume. Neoproterozoic and early Paleozoic correlations in the western Ogilvie Mountains. *In: Yukon Exploration and Geology 2010, K.E. MacFarlane, L.H. Weston and C. Relf (eds.), Yukon Geological Survey.*
- Medig, K.P.R., Thorkelson, D.J. and Dunlop, R.L., 2010. The Proterozoic Pinguicula Group: Stratigraphy, contact relationships and possible correlations. *In: Yukon Exploration and Geology 2009, K.E. MacFarlane, L.H. Weston and L.R. Blackburn (eds.), Yukon Geological Survey, p. 265-278.*
- Morrow, D.W., 1999. Lower Paleozoic stratigraphy of northern Yukon Territory and Northwestern District of Mackenzie. Geological Survey of Canada, Bulletin 538.

- Murphy, D. C., 1997. Geology of the McQuesten river Region, Northern McQuesten and Mayo Map Areas, Yukon Territory (115P/14, 15,16; 105M/13, 14).
- Nielsen, A.B., Thorkelson, D.J., Marshall, D.D. and Gibson, H.D., 2011, this volume. Paleoproterozoic Bonnet Plume River intrusions: Evidence for a calc-alkaline arc at 1.7 Ga and its partial preservation in Yukon, Canada. *In: Yukon Exploration and Geology 2010*, K.E. MacFarlane, L.H. Weston and C. Relf (eds.), Yukon Geological Survey.
- Peters, T.J. and Thorkelson, D.J., 2011, this volume. Volcano-sedimentary megaclast in Wernecke breccia, Yukon, and its bearing on the Proterozoic evolution of northwestern Laurentia. *In: Yukon Exploration and Geology 2010*, K.E. MacFarlane, L.H. Weston and C. Relf (eds.), Yukon Geological Survey.
- Roots, C.F., 2003. Bedrock geology of Lansing Range map area (NTS 105N), central Yukon (1:250 000-scale). Yukon Geological Survey, Energy Mines and Resources, Government of Yukon, Geoscience Map 2003-1; and Geological Survey of Canada, Open File 1616.
- Roots, C.F., 1997. Bedrock geology of Mayo map area, central Yukon (105M). Exploration and Geological Services Division, Indian and Northern Affairs Canada, Geoscience Map 1997-1, 1:50 000 scale.
- Tempelman-Kluit, D.J., 1977. Stratigraphy and structural relations between the Selwyn basin, Pelly Cassiar Platform, and Yukon Crystalline Terrane in the Pelly Mountains, Yukon. *In: Report of Activities, Part A; Geological Survey of Canada, Paper 79-14*, 27 p.
- Thompson, R.I., Roots, C.F. and Mustard, P.S., 1992. Geology of Dawson map area (116B, C) (northeast of Tintina Trench). Geological Survey of Canada, Open File 2849, 13 sheets, scale 1:50 000.
- Thorkelson, D.J., 2000. Geology and mineral occurrences of the Slats Creek, Fairchild Lake and "Dolores Creek" areas, Wernecke Mountains (106D/16, 106C/13, 106C/14), Yukon Territory. Exploration and Geological Services Division, Yukon Region, Indian and Northern Affairs Canada, Bulletin 10, 73 p.
- Turner, E.C., 2011, this volume. Stratigraphy of the Mackenzie Mountains supergroup in the Wernecke Mountains, Yukon. *In: Yukon Exploration and Geology 2010*, K.E. MacFarlane, L.H. Weston and C. Relf (eds.), Yukon Geological Survey.
- Yukon MINFILE, 2010. Yukon MINFILE – A database of mineral occurrences. Yukon Geological Survey, <http://www.geology.gov.yk.ca/databases_gis.html>.

Appendix 1

Sample	UTM Zone	UTM Easting	UTM Northing	Mo	Cu	Pb	Zn	Ag	Ni	Co	Mn	Fe	As	U	Au	Th	Sr	Cd	Sb	Bi	V	Ca
10CYA-NG001	8	555554	7099772	2.4	44.3	34.6	158	0.1	66	33.6	710	4.78	17.2	1.1	2.1	3.2	29	0.4	1.2	0.4	29	0.12
10CYA-NG002	8	555547	7099829	1.9	220.6	12.7	170	0.2	87.1	51	1223	9.89	7.7	1	4.8	2.3	20	0.4	1.9	0.1	190	0.38
10CYA-NG003	8	555562	7099955	13.8	433.5	118.5	209	0.5	155.3	81.6	1769	13.47	8.8	5.5	18.1	13.1	89	0.8	1.9	0.2	64	0.22
10CYA-NG004	8	555658	7100244	1.7	37.2	39.6	72	0.1	20.9	2.6	151	4.44	16.6	1	0.9	7.6	24	0	0.6	0.4	24	0.08
10CYA-NG005	8	555648	7100744	3.8	53.6	32	101	0.7	47.4	17.1	474	6.61	26.7	1.5	3.6	3.6	47	0.3	2.1	0.3	57	0.12
10CYA-NG006	8	556054	7099748	2.2	34.7	24.1	91	0.1	41.2	15.7	384	4.29	16	1	1.9	5.6	18	0.3	1.1	0.3	51	0.13
10CYA-NG007	8	556429	7099415	2.9	24.6	29.2	80	0	31	9.7	211	4.33	18.1	0.8	2.6	4.9	24	0.2	0.9	0.4	42	0.04
10CYA-NG008	8	556876	7099189	3.4	41.2	39	177	0.2	91.7	34	850	5.3	20.3	1.7	1.1	8.4	65	0.6	1.1	0.5	33	0.12
10CYA-NG009	8	557241	7099531	4.6	57.7	37.4	78	0.1	27	7	308	4.29	17.1	1.1	0.9	5.6	39	0.1	0.7	0.5	18	0.02
10CYA-NG010	8	555056	7099850	2.3	34.2	35.6	101	0.1	50.5	15.6	245	4.35	15.9	1.1	1.2	6.1	24	0.2	0.7	0.4	23	0.09
10CYA-NG011	8	552059	7100147	2.5	31.7	12.2	69	0	25.2	8.8	397	2.99	9.4	0.8	2.4	1.6	13	0.3	0.7	0.2	72	0.16
10CYA-NG012	8	552548	7099893	2.6	21.5	13	60	0	16.8	5.5	239	3.08	12.1	0.8	2.4	0.7	10	0.2	0.9	0.3	71	0.07
10CYA-NG013	8	553055	7099691	2.1	25.1	11.9	39	0.1	17.8	5.1	130	2.48	9.6	0.9	0.7	0.3	10	0.5	0.7	0.2	57	0.06
10CYA-NG014	8	553830	7099679	6	36	15.8	69	0.2	22.5	8.2	285	3.07	12.5	2.1	2.8	0.5	25	0.4	0.9	0.3	62	0.07
10CYA-NG015	8	554089	7099567	14.3	96.6	52.8	151	0.5	51.8	28.3	1231	6.77	31.9	2.7	0.8	7.3	52	0.7	1.6	0.4	46	0.26
10CYA-NG016	8	554568	7099968	3.3	44.9	34.1	107	0.1	52.7	21.2	525	4.08	19	1.1	1.8	3.1	25	0.3	1.1	0.4	32	0.17
10CYA-NG017	8	554365	7100425	2.2	82.2	26	89	0.7	38.2	6.9	227	3.32	11.3	1.2	8.1	1.3	23	0.2	1.3	0.4	35	0.02
10CYA-NG018	8	554348	7100925	6	102.2	63.8	578	0.4	60.2	22.2	575	5.19	34.3	1.8	3.3	1.1	17	2.6	2.7	0.6	135	0.1
10CYA-NG019	8	553894	7101139	3.3	248.3	11.2	846	0.2	81.5	109.7	1315	10.9	864.6	0.6	21.5	2.5	13	3	14	0.3	284	0.21
10CYA-NG020	8	555535	7099271	20.2	79.3	53.2	180	0.4	65.8	51.8	3379	6.7	32.7	2.7	3.8	3.7	44	1.5	2.2	0.3	46	0.15
10CYA-NG021	8	555554	7099772	2.1	43.8	31.2	136	0.1	56.3	31.1	624	4.24	17.5	1.2	1.8	4.1	28	0.4	1.2	0.3	28	0.14
10CYA-NG022	8	556078	7109829	7.9	29.2	23.4	94	0.4	18.1	4.2	130	3.25	28.9	1.2	2	1.4	17	0.2	7.7	0.3	49	0.04
10CYA-NG023	8	553723	7108963	1.7	43.3	14.7	67	0.4	21.7	5.5	161	3.05	12.3	0.9	2.9	1	24	0.2	1.2	0.3	47	0.06
10CYA-NG024	8	554105	7109456	1.9	73.5	18.3	72	1.5	21.2	6.5	156	3.65	21.5	0.8	5	3.4	13	0.2	1.7	0.2	57	0.05
10CYA-NG025	8	554651	7109347	3.5	64.7	21.9	83	0.8	27.4	6	200	2.83	14.7	1.2	9.9	0.5	16	0.2	2.2	0.3	52	0.03
10CYA-NG026	8	555281	7109216	6.1	26.2	22.9	37	1.4	8.9	2.3	97	3.1	19.3	1.2	3.4	0.6	24	0.2	3.2	0.4	51	0.02
10CYA-NG027	8	555882	7109368	2	29.3	15.7	104	0.1	31.5	10.2	345	2.9	15.5	1.1	1.9	2.1	16	0.4	1.6	0.2	46	0.12
10CYA-NG028	8	556092	7108913	3.7	88	17.2	200	1.4	99.5	13.4	1531	4.3	14.4	1.5	9.5	1	22	0.9	2.1	0.2	44	0.17
10CYA-NG029	8	556381	7108503	1.9	29	16.8	95	0.3	23.7	11.2	353	2.93	14.5	1.5	3	2.5	14	0.2	1.2	0.3	57	0.14
10CYA-NG030	8	556078	7109829	8.4	31	24.3	102	0.4	18	4.2	114	3.34	31.2	1.3	2	1.7	18	0.2	8.5	0.3	51	0.04
10CYA-NG031	8	558171	7109448	2.6	15.1	18.2	61	0.2	15.1	5.6	249	3.23	13.6	0.8	1.3	1.1	8	0.2	1.4	0.4	71	0.05
10CYA-NG032	8	557969	7109906	6	41.3	35.5	43	0.1	9.3	1.6	63	3.42	26.4	0.9	1.7	1.8	14	0	6.1	0.5	35	0.01
10CYA-NG033	8	557481	7110031	2	20.7	18.7	79	0	21.4	8.1	308	2.83	14	1	1.6	1.4	11	0.3	2.1	0.3	47	0.06
10CYA-NG034	8	556982	7110086	4.1	22.3	16.9	83	0.6	20.9	8.2	301	2.92	20.8	1.1	2.7	0.9	14	0.4	8.2	0.3	61	0.09
10CYA-NG035	8	556526	7110298	6	60.8	44.5	108	0.4	35.8	2.1	83	4.71	33.5	1.6	0.6	4.2	21	0.6	4.8	0.5	42	<0.01
10CYA-NG036	8	555588	7109939	12.2	41.2	31.2	90	0.3	14.4	2.1	63	3.17	36.9	2	0.8	4.2	19	0.2	12	0.4	44	0.01
10CYA-NG037	8	554873	7108301	2.3	46.3	23.7	76	0.5	24.4	7.9	457	3.5	13.4	0.8	3.4	1.4	8	0.2	1.2	0.4	56	0.06
10CYA-NG038	8	554927	7108863	2.5	33.9	19	80	0.2	22.6	8.8	405	3.42	14.2	0.8	2.6	1.3	10	0	1.3	0.4	71	0.08
10CYA-NG039	8	551660	7111926	1	33.4	23.7	66	0	30	10.6	250	3.13	8	0.7	1.7	7	10	0	0.7	0.3	26	0.1

Sample	UTM Zone	UTM Easting	UTM Northing	Mo	Cu	Pb	Zn	Ag	Ni	Co	Mn	Fe	As	U	Au	Th	Sr	Cd	Sb	Bi	V	Ca
10CYA-NG040	8	552130	7112102	1.3	22.9	21.3	78	0	27.1	9.6	318	2.56	9.9	0.6	1.9	1.6	14	0.2	0.8	0.2	40	0.24
10CYA-NG041	8	552558	7111842	1.4	24.8	85.2	112	0	41.9	20.3	735	4.92	12.4	1	2.7	3.4	15	0	0.8	0.7	20	0.03
10CYA-NG042	8	553036	7111691	1.2	39.8	47.9	80	0	25.8	11.2	407	3.65	14.9	1.7	2.9	1.9	17	0.1	0.9	0.4	25	0.03
10CYA-NG043	8	553495	7111895	1.4	55.4	42.5	96	0	29.7	9.8	248	4.4	13	1.3	2	3.5	17	0.2	0.6	0.5	19	0.02
10CYA-NG044	8	556260	7113044	1.4	34.7	22.5	95	0	27.7	10.8	359	3.24	13.6	1.8	3	1.7	18	0.2	0.8	0.4	53	0.12
10CYA-NG045	8	557258	7112948	1.2	48.4	52.8	69	0	28.2	29.3	954	3.44	13.3	1.5	2.3	3.1	9	0.1	0.7	0.5	30	0.03
10CYA-NG046	8	556415	7113521	1.3	23.5	19.5	80	0	22.8	9.2	423	2.81	8.7	0.7	1.1	0.9	13	0.2	0.6	0.4	32	0.15
10CYA-NG047	8	553855	7115638	0.9	43.4	70.7	98	0	38.3	21.5	1111	4.34	14.4	1.1	0.9	3.4	16	0.1	0.5	0.7	26	0.13
10CYA-NG048	8	555000	7115000	0.3	50.6	24.8	115	0	47	23.4	1469	5.34	10.6	0.8	1.5	5	8	0	0.1	0.6	21	0.07
10CYA-NG049	8	555346	7115474	2.2	34.5	66.4	882	0.2	44	30.5	2168	6.37	37.4	2.1	2.3	3.1	139	0.8	2.2	0.4	15	8.61
10CYA-NG050	8	555424	7115430	1	34.5	29.1	63	0	29	15.8	772	3.65	8.2	1.2	1.5	6.5	16	0	0.4	0.4	12	0.3
10CYA-NG051	8	555819	7115306	1.2	31.9	37.2	68	0.1	22.4	13.6	1212	4.28	5.4	1.5	2.8	3.4	18	0.2	0.4	0.3	16	0.21
10CYA-NG052	8	554848	7115514	1	59.1	41.8	100	0	46.9	23.8	1008	4.11	11.8	0.9	2.5	6.6	65	0	0.7	0.6	14	0.37
10CYA-NG053	8	554300	7115413	1.4	44.4	77.1	87	0.2	42.2	23	1695	3.67	12.8	1.6	4.3	5.9	46	0.3	0.7	0.4	22	0.39
10CYA-NG054	8	550938	7117595	50.2	93.2	45.5	1135	2	875.6	18.4	646	3.36	69.7	11.3	3.7	3	688	12.6	11.1	0.3	574	1.33
10CYA-NG055	8	551013	7117101	6.3	40.8	365.8	324	1.9	19.7	5.4	281	2.54	106.9	1.9	11.4	2.5	37	5.4	27.4	0.3	45	0.08
10CYA-NG056	8	551103	7116608	0.9	47.8	44.3	97	0.3	41.6	21.5	620	3.61	25.3	0.7	2	5.6	19	0.4	1.8	0.6	17	0.23
10CYA-NG057	8	551403	7116208	1	38.8	37.7	61	0.2	39.2	13.6	222	3.23	8.3	1.2	2	5	209	0.2	0.4	0.4	7	4.08
10CYA-NG058	8	551530	7115723	1.1	57.9	28.9	64	0.1	39.6	27.6	576	3.48	9.4	1	1.3	8.1	19	0	0.4	0.7	8	0.23
10CYA-NG059	8	551850	7115541	0.6	40.5	39.9	89	0.1	34.2	18.5	598	3.63	10.1	2.7	2.9	9	26	0	0.6	0.5	7	0.19
10CYA-NG060	8	552363	7115448	1.4	48.5	52.1	79	0.2	40.6	17.7	867	3.67	16.1	1.2	1.5	7.4	169	0.2	0.7	0.6	12	0.4
10CYA-NG061	8	552893	7115363	1.4	50.8	49.9	84	0.1	47.4	19.1	621	3.56	21.4	1.2	0.7	8.5	94	0.1	1.2	0.5	13	0.24
10CYA-NG062	8	553354	7115635	1.7	49.1	45.2	112	0.1	34.9	22.7	280	4.67	9.9	1.5	2.9	5.7	17	0.2	0.8	0.5	21	0.03
10CYA-NG063	8	554258	7114718	0.4	38.1	17.3	96	0	38.9	17.5	515	4.34	1.8	1.3	1.6	6.4	17	0	0.2	0.5	31	0.18
10CYA-NG064	8	554258	7114718	0.4	37.9	18.3	90	0	39.9	17.3	558	4.4	2.5	1.3	2.6	6.7	17	0	0.3	0.5	32	0.18
10CYA-NG065	8	555147	7116809	0.8	40.4	135.2	81	0	45.6	20.8	871	4.26	4	1.4	1.4	6.5	17	0	0.2	0.6	16	0.05
10CYA-NG066	8	555399	7116376	0.6	35.9	53.9	40	0.2	56.3	17.6	348	4.77	9.6	0.5	2.2	8	25	0	0.5	0.4	7	0.59
10CYA-NG067	8	555281	7115890	0.8	50.1	44.6	63	0.1	37.1	23.8	513	3.51	8	1	2.2	7.8	28	0	0.5	0.7	7	0.14
10CYA-NG068	8	552640	7116887	0.7	20.5	67.5	105	0	23.5	30.5	814	5.05	5.4	0.6	1.7	3.2	7	0.2	1.3	0.4	28	0.03
10CYA-NG069	8	552936	7116483	0.6	28.5	29	73	0	26.1	12.4	463	3.33	5.5	1.4	2.5	2.4	12	0	0.3	0.5	28	0.1
10CYA-NG070	8	553280	7116119	0.7	46.4	45.6	89	0	41	23.3	1254	4.6	4.7	0.8	2.6	3.5	14	0	0.3	0.6	23	0.06
10CYA-NG071	8	551722	7122992	1.1	46.3	20.7	68	0	30.9	22.4	846	3.76	6.3	0.7	9.1	2.4	13	0.2	0.8	0.3	48	0.22
10CYA-NG072	8	552229	7123022	1.1	75.3	23.8	80	0.1	39.7	27.6	1093	4.99	4.4	0.6	8.3	3.9	15	0.2	0.7	0.3	47	0.24
10CYA-NG073	8	552728	7123081	0.7	43.4	24.6	70	0.1	27.5	13.3	543	4.52	4.2	0.3	5.3	1.7	33	0.2	0.4	0.3	31	2.07
10CYA-NG074	8	554209	7123083	0.9	32.4	7.1	101	0	76.2	30.2	753	4.85	12.3	0.4	1.3	2.1	78	0.3	0.3	0	27	5.09
10CYA-NG075	8	553702	7123319	2.9	18.7	50.4	119	0.2	24.1	8	496	1.91	27.2	3.2	2.1	2.8	53	0.5	1.1	0.2	30	11.49
10CYA-NG076	8	550720	7122939	1.1	19.3	35.9	85	0.2	22.2	11.6	797	3.17	12.8	0.6	1.7	1.4	22	0.4	1.1	0.2	36	2.41
10CYA-NG077	8	551063	7122930	3.1	11.2	34.1	80	0	10.4	4.6	334	0.95	5	0.3	2.4	0.7	194	0.3	3.1	0	16	11.64
10CYA-NG078	8	553213	7123210	0.2	16.9	13.1	49	0	21.4	8.1	253	1.52	2.1	1.8	1.6	6.6	83	0	0.2	0.2	10	6.92
10CYA-NG079	8	557470	7116239	0.9	26	26.4	48	0	27.8	15.3	1305	3.22	6.4	0.7	2.1	5.2	7	0.1	0.4	0.3	23	0.07
10CYA-NG080	8	557508	7116738	2	22.2	23.5	62	0	22.2	9.5	441	3.09	15.1	1	2.6	4.1	21	0.4	0.7	0.3	36	0.25

Sample	UTM Zone	UTM Easting	UTM Northing	Mo	Cu	Pb	Zn	Ag	Ni	Co	Mn	Fe	As	U	Au	Th	Sr	Cd	Sb	Bi	V	Ca
10CYA-NG081	8	557900	7114198	0.6	28.9	22	53	0	18.3	4.2	123	3.13	5.4	0.8	0.8	3.6	13	0	0.3	0.3	15	0.03
10CYA-NG082	8	557400	7114159	1.2	25.8	43.6	29	0.2	51	16.9	297	2.32	7.2	0.8	1.7	3.8	32	0	0.3	0.3	7	0.92
10CYA-NG083	8	557124	7114579	0.9	40.4	36.4	78	0	38.6	28.4	1258	3.74	13	1.5	2.1	4.4	22	0.1	0.7	0.4	19	0.14
10CYA-NG084	8	558454	7117413	0.9	59.1	26.2	82	0	27.8	17.3	959	3.62	15.3	0.5	2.3	2.7	15	0.2	0.4	0.4	18	0.4
10CYA-NG085	8	558868	7117130	1.2	24.8	32.6	53	0	20.3	19.4	1461	3.5	9.6	0.8	2.9	1.6	9	0.1	0.6	0.4	31	0.03
10CYA-NG086	8	559135	7116707	1.6	27.7	26.3	65	0	23.1	12	486	3.62	9.2	0.8	1.1	1.2	9	0.1	0.8	0.5	42	0.04
10CYA-NG087	8	559608	7116542	1	29.1	40.3	77	0	28.8	20.1	1106	3.65	8.8	0.8	2	3.1	10	0.1	0.6	0.4	32	0.06
10CYA-NG088	8	559629	7116041	1.4	96.8	34.8	67	0	37.6	22.6	2920	3.71	13	1.2	1.7	2.2	32	0.2	0.4	0.4	17	0.64
10CYA-NG089	8	559395	7115597	1.2	40.9	30.2	74	0.1	31.3	13.9	347	3.56	14.7	0.5	1.4	3.5	42	0.1	0.6	0.3	17	0.11
10CYA-NG090	8	550361	7114201	0.5	23.8	21.6	52	0.1	24.9	9.1	239	2.15	5.8	0.4	2.1	4.2	85	0	0.3	0.2	8	1.97
10CYA-NG091	8	550147	7111460	1.1	4.3	28	11	0	3.4	0.4	10	1.21	8.7	0.3	1.9	3.2	5	0	0.8	0.6	5	<0.01
10CYA-NG092	8	553910	7112175	1.9	31.5	21.5	61	0	20.9	8.3	274	2.79	10.1	0.9	2.4	1	10	0.1	0.7	0.3	36	0.06
10CYA-NG093	8	564977	7113381	0.8	27.3	19.3	53	0	26.8	16.1	1253	2.75	6.9	0.8	2.2	2.1	46	0	0.5	0.3	19	2.08
10CYA-NG094	8	564545	7113681	1.5	48	47.1	90	0.2	17.2	6.8	318	5.47	14	0.8	1.5	7.3	55	0	0.6	0.5	17	0.19
10CYA-NG095	8	564107	7114000	1.2	19.2	15.2	64	0	24.2	8.4	285	2.51	8.3	0.7	3.6	1.9	14	0.2	0.9	0.2	38	0.14
10CYA-NG096	8	563628	7114202	1.3	25.3	27.9	137	0.2	39.9	16.1	875	3.37	8.5	0.7	5.2	3.3	28	0.3	0.7	0.3	31	0.3
10CYA-NG097	8	563124	7114426	1.2	21	25	45	0	23.5	9.6	254	2.52	9.7	0.5	1.7	2.1	13	0	0.6	0.3	30	0.06
10CYA-NG098	8	562627	7114333	0.7	35.3	33.9	91	0.1	59.1	20.4	857	3.76	11.5	1	2	4.1	23	0	0.4	0.3	17	0.53
10CYA-NG099	8	562126	7114329	1	26.2	15.4	68	0	21.5	8.6	280	2.54	8.2	1.3	3	3.6	15	0.1	0.6	0.2	32	0.13
10CYA-NG100	8	561639	7114452	0.9	37.5	62	84	0	36.7	20.6	762	3.53	13.2	1.3	3.5	3.7	25	0.2	0.6	0.5	21	0.07
10CYA-NG101	8	561183	7113987	0.7	13.6	19.6	81	0	33.2	14.8	422	3.57	2.2	0.7	1.5	2.3	5	0.1	0.4	0.4	27	0.03
10CYA-NG102	8	563689	7116866	0.7	30.4	40.4	101	0	38.1	16.4	816	4.89	13.9	0.7	1.4	4.4	9	0	0.3	0.6	23	0.04
10CYA-NG103	8	563667	7116358	0	4.4	2.1	12	0	1790.5	89.7	405	2.89	0.6	0	1.7	0	0	0	0.1	0	11	<0.01
10CYA-NG104	8	563713	7115812	0.8	142	13.4	103	0	56.7	39.4	1178	6.79	13.4	0.4	5.7	2.4	9	0.2	0.6	0.2	64	0.08
10CYA-NG105	8	563838	7115126	0.9	58.5	22.4	38	0.1	13.2	16.2	1159	3.95	3.5	0.8	2.4	0.8	5	0.1	0.4	0.5	23	0.03
10CYA-NG106	8	563761	7115066	0.4	27.3	24.7	57	0	18.2	12.9	360	2.37	5.3	2.6	2	3	27	0	0.3	0.5	16	0.58
10CYA-NG107	8	563532	7114763	1.1	21.8	19.8	53	0	12.8	7.6	349	2.46	6.6	0.7	3.1	1.3	6	0	0.5	0.3	33	0.02
10CYA-NG108	8	562315	7115704	1.3	23.4	32.2	66	0	23.5	14.5	558	3.35	12.5	0.7	3.1	4.4	7	0.2	0.7	0.4	38	0.03
10CYA-NG109	8	571298	7115570	0.7	950.1	5.5	323	0	2254.4	250.7	2615	10.12	3.1	0.2	11.3	1	5	1.6	0.1	0.4	37	0.03
10CYA-NG110	8	571139	7115096	0.7	35	35.6	90	0.1	52.8	15.9	707	4.32	18.3	2.3	1.7	6.2	23	0.1	0.6	0.4	23	0.26
10CYA-NG111	8	567617	7116283	1.2	26.1	18.7	59	0	20.2	13.3	469	3.02	6.2	0.6	0.7	5	5	0.2	0.7	0.4	34	0.02
10CYA-NG112	8	567613	7115781	4.4	102.7	31	98	0.1	51.8	30.5	948	5.61	23.3	0.3	2.4	2.2	26	0.4	1.1	0.5	15	1.48
10CYA-NG113	8	567628	7115282	1.5	43.8	15.5	74	0	80.2	28.2	1059	4.98	7.2	0.6	1.1	3.2	13	0.3	0.5	0.2	32	0.19
10CYA-NG114	8	567689	7114782	1.1	21.2	19.6	50	0.2	21	8.6	375	2.14	20.5	2.3	2.5	1.3	485	0.3	0.8	0.2	25	6.48
10CYA-NG115	8	567563	7114270	1.6	24.2	25.8	67	0	20.5	11.1	625	3.51	11.1	0.8	1.9	0.7	7	0.1	0.8	0.4	47	0.05
10CYA-NG116	8	568901	7114113	0.8	45.2	48.3	148	0	34.3	19.6	962	4.2	8.1	1.2	1.5	5.2	12	0.1	0.4	0.6	14	0.06
10CYA-NG117	8	567644	7113777	1	25.9	23.3	67	0	24	12.4	436	3.5	7.1	0.7	1.4	1.9	9	0.2	0.5	0.5	34	0.04
10CYA-NG118	8	567644	7113777	0.9	31.5	27.6	77	0	30	15.4	525	3.84	8.7	0.9	1.7	3.8	10	0.2	0.6	0.5	29	0.05

Sample	P	La	Cr	Mg	Ba	Ti	B	Al	Na	K	W	Hg	Sc	Tl	S	Ga	Se	Te
10CYA-NG001	0.135	15	24	0.3	81	0.007	3	1.03	0.007	0.06	0.1	0.06	2.3	0.2	<0.05	3	1.1	<0.2
10CYA-NG002	0.112	12	64	1.35	331	0.024	2	3.32	0.005	0.03	0	0.61	18.4	0	<0.05	10	0.9	<0.2
10CYA-NG003	0.302	54	52	1	207	0.016	3	3.49	0.081	0.1	0	0.14	8.4	0.3	0.38	7	3.9	0.4
10CYA-NG004	0.091	25	35	0.66	177	0.002	2	1.46	0.013	0.11	0	0.07	1.9	0.2	0.23	5	0.5	<0.2
10CYA-NG005	0.409	20	47	0.68	274	0.044	3	2.06	0.019	0.08	0.4	0.05	3.5	0.2	0.13	6	3	<0.2
10CYA-NG006	0.075	22	39	0.56	105	0.018	3	2.41	0.007	0.07	0.2	0.06	3	0.2	<0.05	6	1.1	<0.2
10CYA-NG007	0.066	15	29	0.42	77	0.016	2	1.29	0.008	0.07	0.1	0.03	2.2	0.2	0.08	6	0.6	<0.2
10CYA-NG008	0.125	19	39	1.18	57	0.002	2	2.29	0.017	0.12	0	0.09	2.5	0.5	0.24	6	1.3	<0.2
10CYA-NG009	0.108	27	39	0.33	133	0.002	3	0.99	0.017	0.08	0	0.3	1.4	0.2	0.15	4	1.2	<0.2
10CYA-NG010	0.081	34	31	0.49	140	0.002	2	1.59	0.008	0.08	0	0.11	2.4	0.2	0.08	5	0.7	<0.2
10CYA-NG011	0.081	14	35	0.43	136	0.05	2	1.34	0.007	0.05	0.2	0.04	2.2	0	<0.05	6	0.7	<0.2
10CYA-NG012	0.063	13	29	0.3	92	0.032	2	1.46	0.006	0.06	0.2	0.05	1.4	0.1	0.05	7	0.6	<0.2
10CYA-NG013	0.085	12	29	0.27	129	0.015	2	1.57	0.008	0.05	0.2	0.06	0.9	0.1	0.06	6	0.8	<0.2
10CYA-NG014	0.126	19	34	0.43	139	0.025	2	1.76	0.012	0.05	0.2	0.06	1.4	0.2	0.12	6	1.4	<0.2
10CYA-NG015	0.205	39	42	0.87	171	0.126	2	1.78	0.048	0.12	0	0.09	4.3	0.2	0.36	6	2.7	<0.2
10CYA-NG016	0.142	24	46	0.49	107	0.005	2	1.53	0.007	0.09	0	0.04	2.1	0.2	0.08	5	0.7	<0.2
10CYA-NG017	0.109	17	43	0.44	153	0.006	2	1.49	0.008	0.05	0	0.08	1.1	0.1	0.08	5	1	<0.2
10CYA-NG018	0.08	13	42	0.64	163	0.027	2	1.87	0.008	0.05	0.2	0.08	3.1	0.1	0.07	7	3.3	<0.2
10CYA-NG019	0.063	10	34	0.78	261	0.042	2	2.35	0.008	0.06	0.1	0.09	13.7	0.1	<0.05	9	4.4	<0.2
10CYA-NG020	0.187	47	43	0.73	178	0.007	2	1.86	0.045	0.09	0	0.17	2.7	0.4	0.2	5	2.9	<0.2
10CYA-NG021	0.123	16	24	0.35	89	0.009	1	1.1	0.006	0.07	0.1	0.06	2.4	0.2	<0.05	3	0.8	<0.2
10CYA-NG022	0.084	12	25	0.3	149	0.011	1	1.19	0.008	0.05	0.1	0.07	1.2	0.5	<0.05	4	4.1	0.2
10CYA-NG023	0.072	12	26	0.29	134	0.016	2	1.31	0.007	0.05	0.2	0.08	1.3	0.1	<0.05	5	1.3	<0.2
10CYA-NG024	0.051	11	32	0.31	106	0.032	2	1.63	0.008	0.04	0.2	0.18	1.9	0.1	<0.05	5	1.8	<0.2
10CYA-NG025	0.081	13	30	0.22	143	0.011	1	1.21	0.003	0.05	0.1	0.26	1	0.2	<0.05	5	2.6	<0.2
10CYA-NG026	0.092	19	24	0.13	171	0.008	2	0.76	0.012	0.05	0.1	0.09	0.7	0.2	0.07	5	3.3	<0.2
10CYA-NG027	0.074	12	28	0.49	118	0.027	2	1.75	0.007	0.05	0.2	0.04	2	0.1	<0.05	5	1.1	<0.2
10CYA-NG028	0.093	18	27	0.18	179	0.016	1	1.01	0.005	0.03	0.2	0.54	3.2	0.2	<0.05	3	3.4	<0.2
10CYA-NG029	0.089	18	33	0.58	193	0.034	3	1.86	0.008	0.06	0.3	0.06	2.8	0.2	<0.05	6	0.8	<0.2
10CYA-NG030	0.087	11	24	0.29	159	0.008	2	1.14	0.008	0.05	0.1	0.08	1.2	0.5	0.06	4	4.7	<0.2
10CYA-NG031	0.039	13	28	0.31	77	0.026	1	1.63	0.005	0.04	0.2	0.04	1.5	0.2	<0.05	8	1.2	<0.2
10CYA-NG032	0.053	6	22	0.13	78	0.008	1	0.71	0.004	0.05	0	0.11	0.8	0.4	<0.05	4	2.6	<0.2
10CYA-NG033	0.048	12	28	0.46	106	0.023	2	1.73	0.006	0.05	0.2	0.05	1.8	0.2	<0.05	5	1.2	<0.2
10CYA-NG034	0.068	14	29	0.41	118	0.024	2	1.67	0.009	0.05	0.2	0.07	1.5	0.3	<0.05	6	4.2	<0.2
10CYA-NG035	0.06	3	37	0.65	112	0.004	1	1.63	0.009	0.07	0	0.12	1.9	0.4	0.07	5	2.6	<0.2
10CYA-NG036	0.055	15	20	0.16	105	0.003	1	0.67	0.005	0.05	0	0.09	1.1	0.6	<0.05	3	5.7	<0.2
10CYA-NG037	0.051	12	27	0.31	123	0.021	2	1.39	0.004	0.04	0.2	0.07	1.3	0.1	0.07	5	<0.5	<0.2
10CYA-NG038	0.039	14	34	0.46	168	0.027	2	2.05	0.005	0.04	0.4	0.05	2.4	0.2	<0.05	7	0.8	<0.2
10CYA-NG039	0.032	26	19	0.37	119	0.014	2	1.07	0.004	0.04	0	0.06	2	0	<0.05	3	<0.5	<0.2

Sample	P	La	Cr	Mg	Ba	Ti	B	Al	Na	K	W	Hg	Sc	Tl	S	Ga	Se	Te
10CYA-NG040	0.052	14	22	0.36	125	0.02	4	1.24	0.007	0.04	0.2	0.04	1.6	0	<0.05	3	0.5	<0.2
10CYA-NG041	0.045	7	25	0.62	91	0.007	2	1.58	0.007	0.06	0	0.04	2.2	0	0.06	4	0.5	0.2
10CYA-NG042	0.076	11	27	0.34	81	0.006	2	1.42	0.008	0.1	0	0.08	1	0.1	0.07	4	0.9	<0.2
10CYA-NG043	0.09	6	24	0.47	47	0.002	1	1.62	0.005	0.06	0.1	0.06	1.5	0	<0.05	4	0.9	<0.2
10CYA-NG044	0.06	16	35	0.59	130	0.025	3	2.09	0.007	0.07	0.2	0.05	2.4	0.2	<0.05	6	0.6	<0.2
10CYA-NG045	0.074	26	27	0.41	99	0.006	3	1.5	0.003	0.12	0	0.03	1.3	0.1	0.07	4	<0.5	0.2
10CYA-NG046	0.064	13	24	0.36	75	0.012	2	1.33	0.005	0.06	0.1	0.04	1.3	0.1	<0.05	4	0.6	<0.2
10CYA-NG047	0.075	10	28	0.62	82	0.007	1	1.85	0.004	0.05	0	0.04	2.1	0	<0.05	6	0.5	<0.2
10CYA-NG048	0.023	6	34	1.09	82	0.003	3	2.55	0.008	0.07	0	0.02	4.1	0	<0.05	7	<0.5	<0.2
10CYA-NG049	0.199	14	10	0.45	1118	0.007	3	0.55	0.005	0.06	0	0.9	2.9	0.2	0.1	2	0.7	<0.2
10CYA-NG050	0.05	10	15	0.11	58	0.002	2	0.36	0.003	0.07	0	0.07	2.6	0	<0.05	0	<0.5	<0.2
10CYA-NG051	0.066	7	17	0.12	153	0.005	3	0.48	0.004	0.07	0	0.06	3.5	0	<0.05	1	<0.5	<0.2
10CYA-NG052	0.16	44	15	0.2	49	0.004	2	0.62	0.005	0.07	0	0.42	2.2	0.1	<0.05	2	0.5	0.2
10CYA-NG053	0.089	25	36	0.39	179	0.009	6	1.28	0.005	0.19	0	0.12	2.1	0.1	<0.05	3	0.9	0.2
10CYA-NG054	0.242	15	79	0.39	>10000	0.089	7	1.14	0.006	0.09	0.5	0.21	7.4	6.7	<0.05	3	8.1	<0.2
10CYA-NG055	0.049	14	17	0.21	497	0.011	2	0.68	0.003	0.08	0.1	0.69	1.8	0.2	0.08	2	4.8	<0.2
10CYA-NG056	0.036	18	15	0.13	532	0.003	2	0.63	0.004	0.06	0	0.05	5.2	0	<0.05	2	<0.5	<0.2
10CYA-NG057	0.091	8	10	0.13	63	0.002	2	0.41	0.003	0.06	0	0.43	3.3	0	0.07	0	0.7	<0.2
10CYA-NG058	0.04	5	11	0.32	84	0.005	2	0.83	0.003	0.09	0	0.05	3	0	<0.05	2	<0.5	<0.2
10CYA-NG059	0.047	7	14	0.32	132	0.001	0	0.93	0.003	0.08	0	0.05	2.2	0	<0.05	2	<0.5	<0.2
10CYA-NG060	0.168	23	20	0.31	209	0.004	2	1.04	0.011	0.15	0	0.13	2.6	0.2	0.25	3	0.7	0.2
10CYA-NG061	0.13	14	14	0.14	120	0.005	2	0.79	0.007	0.13	0	0.15	2.7	0.2	0.19	2	0.7	<0.2
10CYA-NG062	0.048	16	16	0.25	53	0.006	2	1.03	0.005	0.05	0	0.1	2.4	0	<0.05	3	<0.5	<0.2
10CYA-NG063	0.035	9	32	0.72	105	0.01	2	1.91	0.015	0.07	0	0.02	4.1	0	<0.05	6	<0.5	<0.2
10CYA-NG064	0.042	9	32	0.71	108	0.009	2	1.81	0.01	0.06	0	0.02	3.7	0	<0.05	6	<0.5	<0.2
10CYA-NG065	0.031	11	22	0.57	58	0.001	2	1.64	0.005	0.06	0	0.04	3.2	0	<0.05	5	<0.5	<0.2
10CYA-NG066	0.113	27	12	0.33	39	0.001	2	0.82	0.002	0.08	0	0.35	2.4	0	<0.05	2	<0.5	<0.2
10CYA-NG067	0.041	3	12	0.13	74	<0.001	2	0.37	0.006	0.1	0	0.04	2.9	0	0.07	0	<0.5	<0.2
10CYA-NG068	0.035	5	19	0.12	99	0.01	0	0.74	0.004	0.04	0	0.03	2.5	0	<0.05	2	<0.5	<0.2
10CYA-NG069	0.067	8	23	0.45	143	0.004	1	1.64	0.007	0.05	0	0.04	2.6	0	0.07	5	<0.5	<0.2
10CYA-NG070	0.058	4	28	0.64	118	0.005	1	1.63	0.005	0.06	0	0.07	2	0	0.05	5	<0.5	<0.2
10CYA-NG071	0.049	13	28	0.83	151	0.021	2	1.65	0.006	0.07	0.1	0.06	3.9	0	0.05	5	<0.5	0.2
10CYA-NG072	0.046	15	28	1.31	285	0.013	2	2.01	0.004	0.06	0	0.1	6.5	0	<0.05	5	<0.5	<0.2
10CYA-NG073	0.062	8	20	1.75	92	0.005	5	1.49	0.006	0.12	0	0.05	5.9	0.1	<0.05	4	<0.5	<0.2
10CYA-NG074	0.151	25	32	0.48	176	0.004	4	0.8	0.008	0.23	0	0.02	7.2	0.2	0.38	3	<0.5	<0.2
10CYA-NG075	0.04	5	14	6.43	34	<0.001	2	0.17	0.017	0.04	0	0.16	2.3	0.9	<0.05	0	<0.5	<0.2
10CYA-NG076	0.057	12	26	1.54	197	0.01	3	1.11	0.007	0.05	0.1	0.08	3.7	0	<0.05	3	<0.5	<0.2
10CYA-NG077	0.035	2	7	7.2	63	0.004	7	0.24	0.014	0.03	0	0.21	2.2	0	<0.05	0	<0.5	<0.2
10CYA-NG078	0.054	16	20	0.94	173	0.008	3	0.66	0.005	0.13	0	0	2.8	0	<0.05	2	<0.5	<0.2
10CYA-NG079	0.035	13	23	0.39	84	0.006	1	1.56	0.005	0.06	0	0.04	2.3	0	<0.05	3	<0.5	<0.2
10CYA-NG080	0.023	12	18	0.22	148	0.006	2	1.24	0.005	0.04	0.1	0.1	2.8	0.1	<0.05	3	<0.5	0.4

Sample	P	La	Cr	Mg	Ba	Ti	B	Al	Na	K	W	Hg	Sc	Tl	S	Ga	Se	Te
10CYA-NG081	0.029	6	21	0.51	54	0.002	0	1.29	0.004	0.05	0	0.02	1.3	0	<0.05	4	<0.5	<0.2
10CYA-NG082	0.093	16	11	0.11	57	0.004	0	0.66	0.006	0.08	0	0.07	2.2	0	<0.05	0	<0.5	<0.2
10CYA-NG083	0.07	9	19	0.37	79	0.008	1	1.12	0.005	0.07	0	0.03	2.4	0	<0.05	3	<0.5	<0.2
10CYA-NG084	0.048	9	10	0.16	180	0.003	3	0.64	0.005	0.06	0	0.08	5.1	0	<0.05	2	<0.5	0.4
10CYA-NG085	0.064	10	23	0.25	86	0.008	1	1.25	0.006	0.12	0	0.04	1.3	0.1	<0.05	4	<0.5	<0.2
10CYA-NG086	0.05	9	27	0.42	59	0.014	0	1.64	0.006	0.05	0.2	0.05	1.7	0.1	<0.05	6	<0.5	<0.2
10CYA-NG087	0.042	9	27	0.58	54	0.02	0	1.59	0.006	0.04	0.1	0.03	2.7	0	<0.05	6	<0.5	<0.2
10CYA-NG088	0.059	21	14	0.2	144	0.004	2	0.71	0.005	0.1	0	0.06	3.8	0	<0.05	2	<0.5	0.4
10CYA-NG089	0.059	17	16	0.14	98	0.006	0	0.66	0.01	0.07	0	0.46	2.5	0.2	<0.05	2	<0.5	0.3
10CYA-NG090	0.028	15	7	0.12	37	0.004	0	0.39	0.003	0.04	0	0.06	2.4	0	<0.05	0	<0.5	<0.2
10CYA-NG091	0.008	3	4	0.04	278	<0.001	2	0.2	0.004	0.04	0	0.05	0.3	0	<0.05	0	<0.5	<0.2
10CYA-NG092	0.066	8	23	0.34	72	0.011	0	1.22	0.006	0.04	0.2	0.04	1.3	0.1	<0.05	4	0.5	<0.2
10CYA-NG093	0.089	20	14	0.37	122	0.006	1	0.96	0.005	0.07	0	0.05	2.6	0	<0.05	2	<0.5	0.2
10CYA-NG094	0.136	8	26	0.55	80	0.002	0	1.32	0.008	0.07	0	0.07	2.2	0.1	0.06	5	0.8	<0.2
10CYA-NG095	0.054	14	21	0.38	103	0.02	0	1.2	0.008	0.05	0.2	0.03	2	0.1	<0.05	3	<0.5	<0.2
10CYA-NG096	0.085	21	23	0.44	129	0.016	0	1.2	0.008	0.06	0.1	0.05	3.6	0.1	<0.05	3	<0.5	<0.2
10CYA-NG097	0.033	17	16	0.26	69	0.011	0	0.98	0.005	0.05	0.1	0.02	1.3	0	<0.05	3	<0.5	0.2
10CYA-NG098	0.059	20	22	0.54	85	0.007	3	0.9	0.005	0.06	0	0.04	3	0.1	<0.05	2	<0.5	0.3
10CYA-NG099	0.065	11	23	0.45	98	0.027	0	1.19	0.007	0.05	0.1	0.04	2.3	0	<0.05	4	<0.5	<0.2
10CYA-NG100	0.041	6	29	0.49	132	0.008	0	1.3	0.007	0.08	0	0.04	2.1	0	<0.05	4	<0.5	<0.2
10CYA-NG101	0.048	4	24	0.6	45	0.009	0	1.25	0.005	0.05	0	0.02	1	0	<0.05	4	<0.5	<0.2
10CYA-NG102	0.047	6	31	0.86	32	0.003	0	2.36	0.006	0.04	0	0.02	2.5	0	<0.05	8	<0.5	<0.2
10CYA-NG103	0.003	0	612	18.58	5	0.002	45	0.22	0.003	<0.01	0	0	3.8	0	<0.05	0	<0.5	<0.2
10CYA-NG104	0.053	11	25	0.55	315	0.005	1	1.48	0.004	0.06	0	0.12	7.7	0	<0.05	4	<0.5	0.4
10CYA-NG105	0.145	3	21	0.14	58	0.005	2	1.14	0.006	0.11	0	0.1	0.8	0.1	0.09	5	<0.5	<0.2
10CYA-NG106	0.068	16	13	0.19	98	0.003	0	1.08	0.005	0.17	0	0.03	2.1	0	<0.05	3	<0.5	<0.2
10CYA-NG107	0.046	8	16	0.17	51	0.007	0	0.9	0.005	0.09	0	0.02	0.9	0.1	<0.05	4	<0.5	<0.2
10CYA-NG108	0.027	8	23	0.4	47	0.012	0	1.59	0.006	0.04	0.1	0.04	2	0	<0.05	6	<0.5	<0.2
10CYA-NG109	0.021	4	428	12.4	166	0.007	16	0.43	0.003	0.01	0	0.03	5	0	<0.05	0	<0.5	<0.2
10CYA-NG110	0.028	25	23	0.48	113	0.005	2	1.26	0.003	0.04	0	0.07	5.9	0	<0.05	3	<0.5	0.3
10CYA-NG111	0.029	10	20	0.32	54	0.015	0	1.31	0.003	0.04	0.1	0.05	1.5	0	<0.05	5	<0.5	<0.2
10CYA-NG112	0.051	2	5	0.63	83	0.005	6	0.34	0.003	0.09	0	0.44	8.2	0.2	0.05	1	0.6	<0.2
10CYA-NG113	0.09	19	21	0.24	123	0.005	1	1.35	0.003	0.06	0	0.04	5.6	0.1	<0.05	4	<0.5	<0.2
10CYA-NG114	0.227	15	17	0.31	111	0.011	3	0.85	0.008	0.05	0.1	0.26	1.7	0	<0.05	2	<0.5	<0.2
10CYA-NG115	0.058	8	27	0.39	47	0.015	0	1.69	0.004	0.05	0.1	0.03	1.3	0	<0.05	7	0.5	<0.2
10CYA-NG116	0.036	7	18	0.38	67	0.003	4	1.13	0.004	0.06	0	0.08	2.9	0	<0.05	3	<0.5	<0.2
10CYA-NG117	0.047	9	23	0.43	51	0.008	0	1.61	0.004	0.05	0	0.02	1.2	0.1	<0.05	6	<0.5	0.2
10CYA-NG118	0.044	9	26	0.53	55	0.008	1	1.78	0.005	0.05	0.1	0.01	1.6	0.1	<0.05	5	<0.5	<0.2

